Leukemia-specific delivery of mutant NOTCH1 targeted therapy

Giovanni Roti,[1,3,4]* Jun Qi,[2]* Samuel Kitara,[1,3] Marta Sanchez-Martin,[5] Amy Saur Conway,[1,3] Anthony C. Varca,[2] Angela Su,[1,3] Lei Wu,[2] Andrew L. Kung,[6] Adolfo A. Ferrando,[5] James E. Bradner,[2,7,8] and Kimberly Stegmaier[1,3,9]

[1]Department of Pediatric Oncology and [2]Department of Medical Oncology, Dana-Farber Cancer Institute, Boston, MA
[3]Division of Hematology/Oncology, Boston Children's Hospital, Boston, MA
[4]Department of Medicine and Surgery, University of Parma, Italy
[5]Institute of Cancer Genetics, Columbia University, New York, NY
[6]Department of Pediatrics, Memorial Sloan Kettering Cancer Center, New York, NY
[7]Department of Medicine, Harvard Medical School, Boston, MA
[8]Novartis Institutes for Biomedical Research, Cambridge, MA
[9]Broad Institute, Cambridge, MA

On-target drug delivery remains a challenge in cancer precision medicine; it is difficult to deliver a targeted therapy to cancer cells without incurring toxicity to normal tissues. The SERCA (sarco-endoplasmic reticulum Ca^{2+} ATPase) inhibitor thapsigargin inhibits mutant NOTCH1 receptors compared with wild type in T cell acute lymphoblastic leukemia (T-ALL), but its administration is predicted to be toxic in humans. Leveraging the addiction of ALL to folic acid, we conjugated folate to an alcohol derivative of thapsigargin via a cleavable ester linkage. JQ-FT is recognized by folate receptors on the plasma membrane and delivered into leukemia cells as a potent antileukemic agent. In mechanistic and translational models of T-ALL, we demonstrate NOTCH1 inhibition in vitro and in vivo. These proof-of-concept studies support the further optimization of this first-in-class NOTCH1 inhibitor with dual selectivity: leukemia over normal cells and NOTCH1 mutants over wild-type receptors. Furthermore, tumor-specific disruption of Notch signaling may overcome legitimate concerns associated with the tumor suppressor function of nontargeted Notch pathway inhibitors.

INTRODUCTION

The successful perturbation of folate metabolism as an approach to treat patients with cancer was first described in a landmark paper in the *New England Journal of Medicine* in 1948. Sidney Farber described the results of the clinical testing of the folate antagonist aminopterin in five children with acute lymphoblastic leukemia (ALL; Farber and Diamond, 1948). That study, for the first time, demonstrated that leukemia cells are highly dependent on folate metabolism while establishing the first reported clinical responses of childhood ALL to drug therapy. Subsequently, the targeting of folic acid metabolism became the foundation of successful ALL treatment.

Folic acid (FA) is a water-soluble vitamin (B9) used as a one-carbon donor in the biosynthesis of the essential purines and thymidylate necessary for the production of DNA and RNA (Fig. 1 A). Folate enters cells by two mechanisms: (1) the reduced folate carrier, a ubiquitously expressed protein with low affinity for folate (Whetstine et al., 2002; Matherly et al., 2007), or (2) folate receptor (FR), which is virtually absent in normal cells but has high affinity for FA (Shen et al., 1997; Kelemen, 2006). The FR family consists of four different proteins: FR1–4 or FRα, β, γ, and δ (Antony, 1992, 1996). Several lines of evidence suggest that FRs are aberrantly expressed in rapidly dividing cells, including cancer cells (Ross et al., 1999; Wang et al., 2000; Lynn et al., 2015). The most extensively characterized FRs in cancer are FR1 and FR2, encoded by the *FOLR* genes located on the long arm of chromosome 11 (q11.3–q13.5). FR1, for example, is overexpressed in several tumors: adenocarcinomas of the ovary, uterus, and pituitary gland and mesothelioma (Garin-Chesa et al., 1993; Parker et al., 2005). Indeed, FR1 expression is 10–100-fold higher in non-mucinous epithelial ovarian tumors than in normal kidney, lung, or breast epithelial cells (Parker et al., 2005; Kalli et al., 2008). FR2, on the other hand, is constitutively expressed in activated macrophages and acute myeloid leukemia (AML; Ross et al., 1999; Wang et al., 2000; Pan et al., 2002; Paulos et al., 2004b; Lynn et al., 2015).

Because of the high dependence of leukemia cells on folate metabolism, we speculated that T-ALL cells might express FRs on their cellular surface. Therefore, T-ALL became an ideal system to further evaluate our drug delivery strategy with the development of a folate-drug conjugate that leverages the

*G. Roti and J. Qi contributed equally to this paper.

Correspondence to Kimberly Stegmaier: kimberly_stegmaier@dfci.harvard.edu; James E. Bradner: james.bradner@novartis.com

The Rockefeller University Press
J. Exp. Med. 2018 Vol. 215 No. 1 197–216
https://doi.org/10.1084/jem.20151778

The Journal of Experimental Medicine

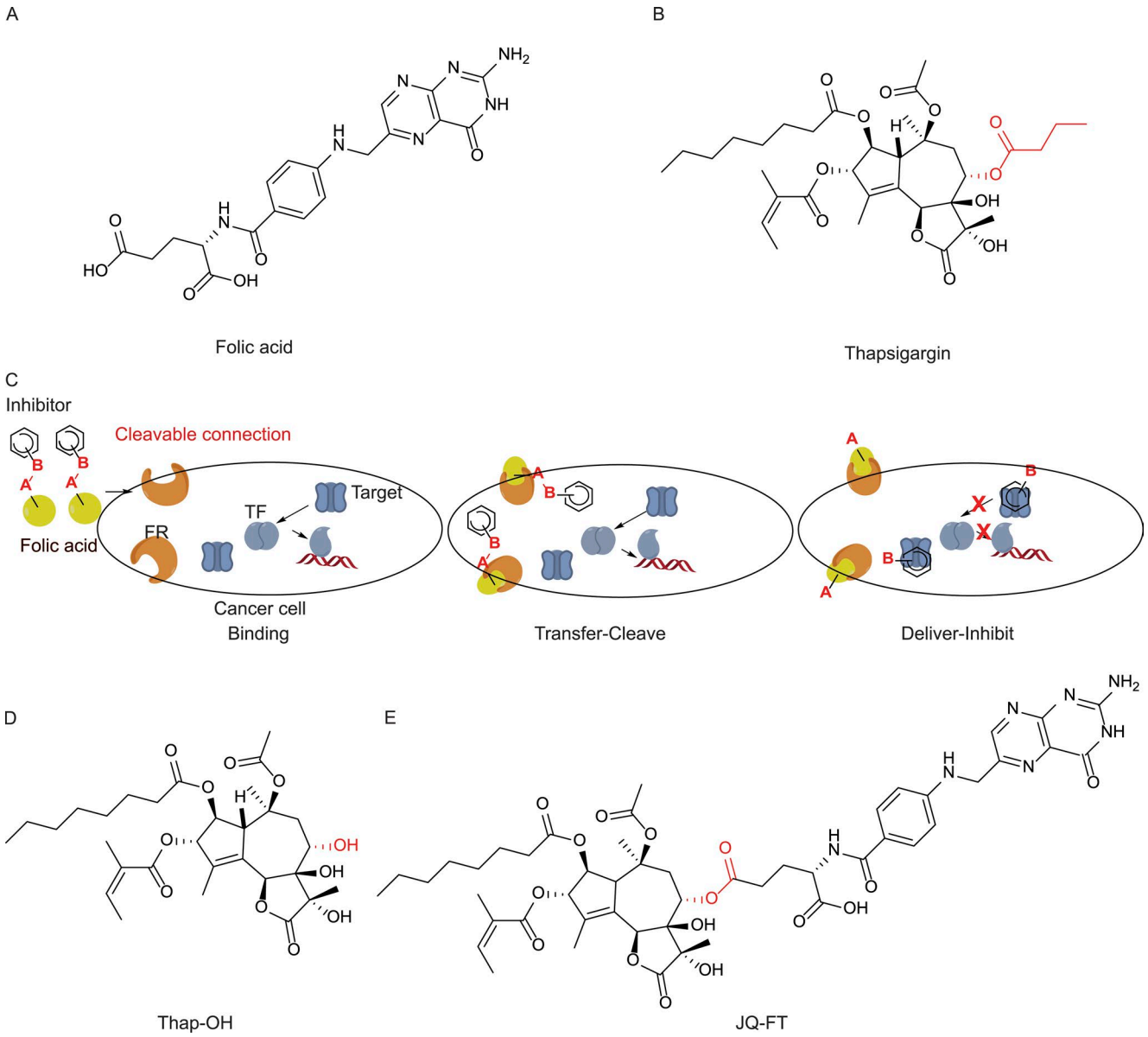

Figure 1. **Design concept of folate-assisted on target drug delivery. (A)** Structure of FA. **(B)** Natural compound thapsigargin as a SERCA inhibitor. **(C)** Design concept for FA-assisted on-target drug delivery. Stage a, the folate derivative selectively binds to cancer cells with overexpression of FR on the cancer cell surface. Stage b, the folate assists the inhibitor entry into the cancer cell, and the cleavable bond is broken and releases the inhibitor motif. Stage c, the inhibitor motif binds to the target and achieves specific target delivery of the inhibitor. **(D)** Structure of 8-*O*-debutanoylthapsigargin, Thap-OH. **(E)** Structure of the designed folate-thapsigargin derivative, JQ-FT.

expression of FR on ALL cells for tumor cell specificity, as well as the activity of a natural product with specificity for mutant NOTCH1, a protein recurrently mutated in this disease.

Folate conjugation has been conceptually advanced as an anticancer strategy by Low and colleagues, who have worked to deliver imaging agents and cytotoxins in a tumor-specific manner for many years (Leamon and Low, 1991, 1994; Leamon et al., 2002; Low and Kularatne, 2009). This concept is borne from the effective clinical use of tumor-localizing strategies to increase the effective molarity of cytotoxic agents on the plasma membrane of tumor cells, notably also including antibody–drug conjugates and nanomaterials (Lee and Low, 1994; Kularatne and Low, 2010; Ab et al., 2015). Despite these advances, to date, folate-conjugated agents have not demonstrated evident clinical utility, which necessitates the ongoing investigation of this strategy. Here, we work to expand the tumor-specific therapeutic index by targeting a folate-addicted cancer with a pathway-specific inhibitor.

In T-ALL, transcription factors play a fundamental role in controlling tumorigenesis, and Notch receptors

(NOTCH1–4) function as ligand-activated transcription factors that mediate a conserved signaling pathway critical in controlling cell fate determination, stem cell quiescence, and differentiation (Tanigaki and Honjo, 2007). Gain- and loss-of-function Notch mutations have been characterized in a constellation of diseases and are frequently observed in cancer (Penton et al., 2012). Moreover, Notch signaling is thought to contribute to chemotherapy resistance (Wang et al., 2014; Takebe et al., 2015). Hence, several studies strongly support the development of Notch inhibition for targeted cancer therapy. This idea is most compelling for T-ALL, where activating mutations of *NOTCH1* are present in 55–60% of cases (Ellisen et al., 1991; Weng et al., 2004), and cancer dependence has been well established (Girard et al., 1996; Capobianco et al., 1997; Aster et al., 2000; Yanagawa et al., 2000; Weng et al., 2004; Beverly et al., 2005; Armstrong et al., 2009; Dail et al., 2010).

Recently, we used gene expression signature, cell-based screens to discover the SERCA inhibitor thapsigargin (Fig. 1 B) as a pathway-specific modulator of mutated NOTCH1 signaling in T-ALL (Roti et al., 2013). This compound had on-target activity in mouse models of human T-ALL, although with efficacy limitations attributable to a narrow therapeutic index. Still, we identified that at thapsigargin concentrations sufficient to inhibit mutant NOTCH1 in vivo, wild-type NOTCH1 and NOTCH2 receptors are properly processed (Roti et al., 2013). This selectivity provides a therapeutic window not observed before with other Notch inhibitors, such as γ-secretase inhibitors or antibody-based approaches, which showed equivalent inhibitory activity against wild-type Notch.

Thapsigargin is a sesquiterpene-γ-lactone isolated from the plant *Thapsia garganica*. Thapsigargin selectively inhibits SERCA, leading to a depletion of ER calcium storage and sustained elevation of cytosolic calcium (Lytton et al., 1991). SERCA channels are critical to maintain intracellular calcium homeostasis in all cell types. Thus, the direct delivery of thapsigargin to animals or humans might be expected to incur cardiac toxicity secondary to calcium ion shifts. We envisioned that the nonspecific toxicity of thapsigargin could be avoided by tagging an active derivative to FA and using a folate-derived drug delivery strategy to take advantage of the specificity of thapsigargin toward mutant NOTCH1. We hypothesized that the compound would bind with FR specifically on T-ALL cells compared with normal cells (Fig. 1 C). The inhibitory motif could be delivered into the cell and cleaved from the folate tag (Fig. 1 C). The released free inhibitory motif could then bind to SERCA in the leukemia cell to block the maturation of mutant NOTCH1 (Fig. 1 C). This strategy could direct the natural product specifically to the cancer cell to further enhance leukemia-specific mutant NOTCH1 inhibition.

RESULTS

Development of folate-conjugated JQ-FT

We designed a folate-thapsigargin derivative based on the following principles: the dual-function molecule should actively bind to FR; the connection between FA and thapsigargin should be stable in serum but cleaved in the intracellular compartment; and the resulting thapsigargin derivative should potently inhibit SERCA activity. We investigated potential anchor sites for installing FA on thapsigargin. Structure–function inferences from the literature suggested that core modifications to appending esters may retain antiproliferative activity (Nielsen et al., 1995; Christensen et al., 1999; Jakobsen et al., 2001; Andrews et al., 2007). The butyl ester bond at C8 was readily, selectively cleaved from the isolated natural product under basic conditions to produce the secondary alcohol, 8-*O*-debutanoylthapsigargin (Thap-OH; Fig. 1 D and Fig. S1). We then connected the carboxylate of FA to the C8-alcohol of Thap-OH to generate the folate conjugate JQ-FT (Fig. 1 E and Fig. S1; see Synthesis of small molecule inhibitors and probes section for full synthetic procedures).

Expression of folate receptor 2 in T-ALL

To establish the expression of folate receptor alleles in human T-ALL, we analyzed the mRNA transcript levels of *FOLR1* and *FOLR2* in 17 T-ALL cell lines and three primary leukemia samples by quantitative RT-PCR. We observed that *FOLR2* was expressed in all leukemia samples, whereas *FOLR1* expression was measurable in only 3/20 cases tested (Fig. 2 A). To confirm stable expression of surface polypeptides, we developed methods for FR1 and FR2 flow cytometry. Because FR isoforms are polypeptides of 220–237 amino acids that share 68–79% sequence identity (Antony, 1996), we first evaluated the specificity of FR antibodies against FR1 and FR2 using a stably transduced *NOTCH1*-mutated T-ALL cell line (RPMI 8402) overexpressing FR1 or FR2 and established the lack of antibody cross-reactivity by flow cytometry (Fig. 2 B). Western blotting of lysates from nine T-ALL cell lines with the isoform-specific FR2 antibody confirmed strong expression of FR2 across all of the samples (Fig. 2 C). We did not observe a significant difference in FR2 levels among *NOTCH1*-mutated (ALL/SIL, DND41, HPB-ALL, KOPTK1, PF382, RPMI 8402) versus wild-type (LOUCY, MOLT16, SUPT11) T-ALL cell lines. These results establish strong expression of FR2.

To assess functional engagement of the folate receptor on T-ALL cells, we generated fluorescence-tagged FA probes, FL-TAMRA and FL-FITC, as tool compounds (Fig. 2 D and Fig. S2). With FL-TAMRA treatment, all tested T-ALL cell lines showed a concentration-dependent increase in fluorescence signal by flow cytometry, notably independent of *NOTCH1* mutational status (Fig. 2 E). T-ALL lines demonstrated stronger FL-FITC labeling compared with T cells isolated from peripheral blood mononuclear cells (PBMCs), providing support for leukemia-specific targeting (Fig. 2 F). Collectively, these observations indicate that functional FR2 expression is increased in T-ALL compared with normal cells, further supporting a rationale for folate-mediated delivery in leukemia.

A

NAME	*FOLR1*	*FOLR2*
ALL/SIL	Y	Y
CCRF-CEM	N	Y
DND41	N	Y
DU528	N	Y
HPB-ALL	N	Y
HSB2	N	Y
JURKAT	N	Y
KOPTK1	N	Y
LOUCY	N	Y
MOLT16	N	Y
MOLT4	N	Y
P12-ICHIKAWA	Y	Y
PEER	N	Y
PF382	N	Y
RPMI 8402	Y	Y
SUPT1	N	Y
SUPT11	N	Y
T-ALL PB#1	N	Y
T-ALL BM#2	N	Y
T-ALL BM#3	N	Y

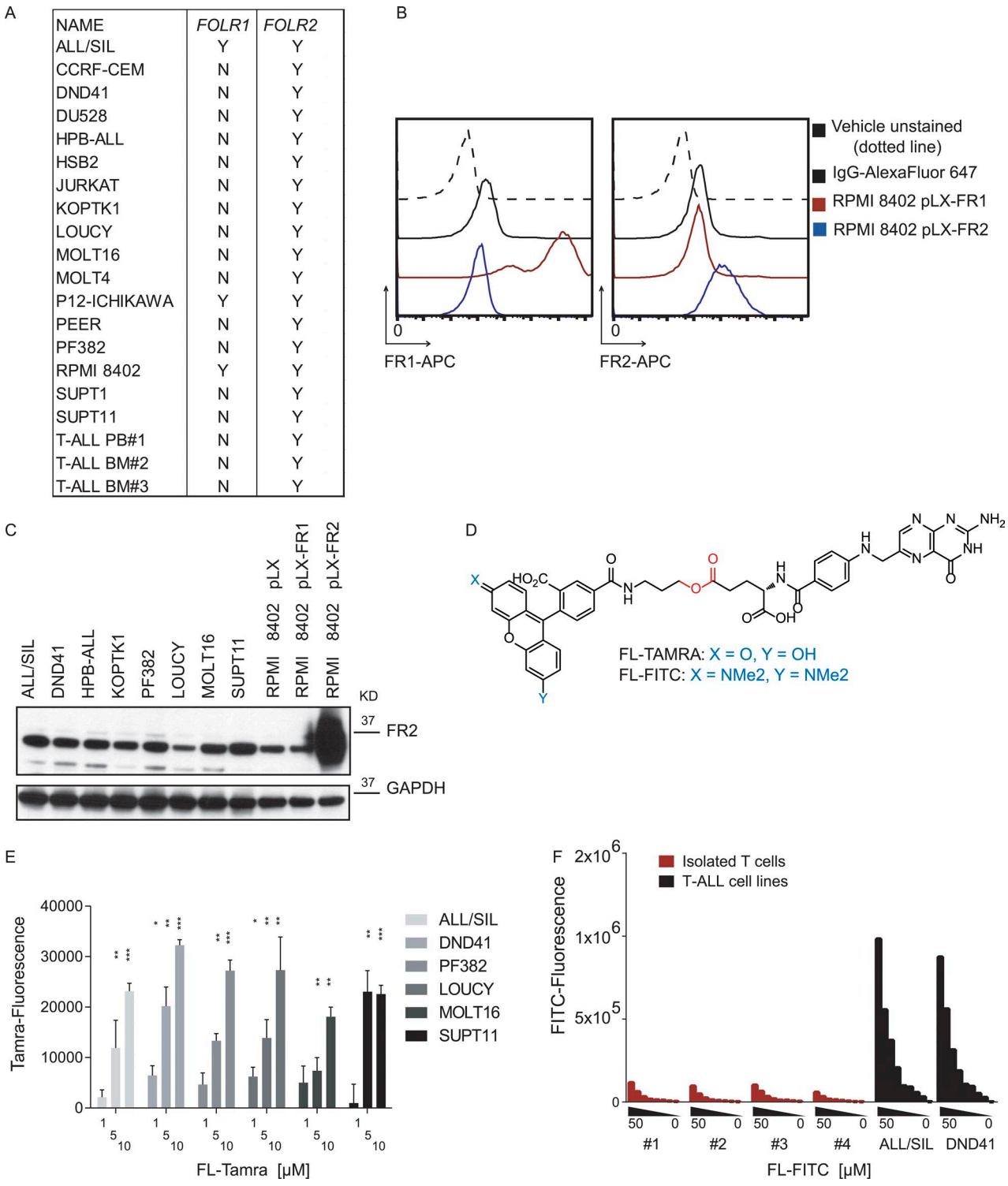

Figure 2. **Folate receptor expression in T-ALL. (A)** Expression of *FOLR1* or *FOLR2* in 17 T-ALL cell lines and three primary human T-ALL samples. Quadruplicate data were collected using quantitative RT-PCR and analyzed using the ΔΔCT method. **(B)** FR1 and FR2 antibodies cross-validation. RPMI 8402 cells stably transduced with a cDNA coding for *FOLR1* or *FOLR2* were stained with FR isoform-specific antibodies. Fluorescence intensity is represented on the x axis. **(C)** FR2 level in T-ALL cell lines. Protein expression is detected using an anti-FR2 antibody. Antibody specificity was confirmed by including the positive control RPMI 8402 pLX-FR2 engineered to stably express high levels of *FOLR2*. **(D)** Structure of FL-TAMRA and FL-FITC. **(E)** Folate uptake in T-ALL cells measured using a TAMRA probe conjugated to FA. T-ALL cells were treated for 6 h with the indicated concentrations of FL-TAMRA. Error bars denote the mean ± SD of three replicates. Statistical significance among the groups for treated vs. vehicle treated (DMSO; *, $P \leq 0.05$; **, $P \leq 0.01$; ***, $P \leq 0.001$) was

Folate conjugates enter T-ALL cells by FR binding and active transport

To explore the mechanism of binding and delivery of folate conjugates in T-ALL, we performed competition and temperature-sensitivity studies of the FL-FITC probe. The T-ALL cell line RPMI 8402 was engineered to overexpress either FR1 or FR2 (Fig. 2 B) and then was treated with increasing concentrations of FL-FITC. We observed a concentration-dependent increase in the FITC signal with overexpression of either FR1 or FR2 (Fig. 3 A). We next addressed whether FA could compete with the FL-FITC probe for uptake. T-ALL cells were grown in medium depleted of FA for 48 h, treated with FL-FITC (1 or 10 μM), and assessed by flow cytometry. T-ALL cells grown in folate-depleted medium exhibited increased fluorescence compared with control cells incubated in standard folate-replete culture conditions (Fig. 3 B) or folate-depleted conditions supplemented with free folate (10 μM; Fig. 3 C). Acidic washing of FL-FITC–incubated cells did not eliminate fluorescence intensity, supporting internalization of the folate conjugate fluorescence probe, as opposed to nonspecific binding to the cell surface (Fig. 3 D).

FL-FITC uptake also showed an energy dependence. T-ALL cells with FR2 overexpression cultured at 4°C were unable to take up FL-FITC. This observation supports an active, endocytic mechanism of uptake, as low temperature blocks endocytosis at 4°C because of altered membrane fluidity (Mamdouh et al., 1996; Punnonen et al., 1998; de Figueiredo and Soares, 2000; Fig. 3 E), in keeping with prior folate-conjugate studies (Leamon and Low, 1991).

FRs are glycosylphosphatidylinositol-anchored membrane proteins associated with caveolar structures (Rothberg et al., 1990; Rijnboutt et al., 1996). To determine whether the endocytic process is mediated by caveolae, we tested FL-FITC uptake in T-ALL cells that were pretreated with filipin, a transient inhibitor of caveolin-mediated endocytosis. The filipin-pretreated T-ALL cells produced significantly reduced FITC fluorescence signal (mean reduction 38.9 ± 2.5%), confirming that the folate conjugate uptake into the cell is mediated by caveolar transport (Fig. 3 F). Together, these results demonstrate that folate-conjugated probes are internalized into T-ALL cells by FR-dependent, caveolae-mediated endocytosis.

Thap-OH inhibits NOTCH1 signaling in T-ALL

To test the hypothesis that Thap-OH targets SERCA in T-ALL cells, we first performed a competitive pull-down assay in which protein lysates were treated with a novel biotinylated derivative of thapsigargin (Thap-biotin in Fig. S3), alone or in the presence of increasing concentrations of free, competitive Thap-OH. Binding to Thap-biotin in a complex mixture was confirmed by immunoblot, as free Thap-OH competed off biotinylated thapsigargin from SERCA2 and SERCA3 (Fig. 4 A).

We previously described that the SERCA inhibitors thapsigargin and cyclopiazonic acid impair NOTCH1 maturation, leading to an accumulation of full-length, unprocessed polypeptides in the ER/Golgi subcellular compartment (Roti et al., 2013). An immediate consequence of SERCA inhibition is a decrement in NOTCH1 protein display on the surface of T-ALL cells. The treatment of T-ALL cells with Thap-OH resulted in a concentration-dependent reduction in NOTCH1 expression on the cell surface by flow cytometry, as was observed with control thapsigargin treatment. Thap-OH was again found to be less potent than the natural product, as predicted from prior studies (Christensen et al., 1993; Jakobsen et al., 2001; Fig. 4 B). To further support the hypothesis that Thap-OH impairs mutant NOTCH1 maturation, we evaluated levels of full-length, transmembrane and activated NOTCH1 (ICN1) by Western blotting. Lysates from T-ALL cell lines treated with 1 μM Thap-OH were immunoblotted with an antibody specific for the cytoplasmic portion of NOTCH1 that recognizes both unprocessed NOTCH1 (FL-N1; ∼270 kD) and the furin-processed transmembrane subunit (TM-N1; ∼110 kD). Consistent with the flow cytometry data, Thap-OH reduced the levels of the furin-processed transmembrane NOTCH1 subunit, but not the unprocessed full-length NOTCH1 precursor, in multiple T-ALL cell lines (Fig. 4 C). Moreover, Thap-OH decreased ICN1 levels in T-ALL cells, suggesting that the cleavage product retains the potent anti-NOTCH1 properties observed with SERCA inhibition.

As expected, treatment with Thap-OH was associated with a decrease in T-ALL cell viability, as measured by dose-ranging ATP content assays (Fig. 4 D). Furthermore, the selectivity for mutant (ALL/SIL, DND41, PF382, RPMI 8402) compared with wild-type (LOUCY, MOLT16, SUPT11) *NOTCH1* was retained with Thap-OH; mutant T-ALL cells were more sensitive to the effects of Thap-OH than *NOTCH1* wild-type cells (Fig. 4 D), and there was no effect on NOTCH1 maturation in the wild-type cell lines at the concentrations tested (Fig. 4, E–G). Thus, cell lines carrying *NOTCH1* alleles with heterodimerization domain mutations were more sensitive to Thap-OH than cells with wild-type *NOTCH1* alleles.

Thapsigargin is a known inducer of the unfolded protein response (UPR). As such, its derivatives may trigger a cellular response that affects the stable expression or trafficking/recycling of folate receptors. FR recycling has variably been reported to take 5.7–20 h in tumor cells, ∼8 h in nor-

determined by one-way ANOVA using Bonferroni's correction for multiple comparison testing. Statistical analysis was calculated using Prism 5 Software (version 6.05). **(F)** Folate uptake in T-ALL cells and T cells isolated from healthy donors. Treatment with indicated concentrations of FL-FITC for 6 h. Absolute FITC quantification from flow cytometric analysis was plotted on y axis.

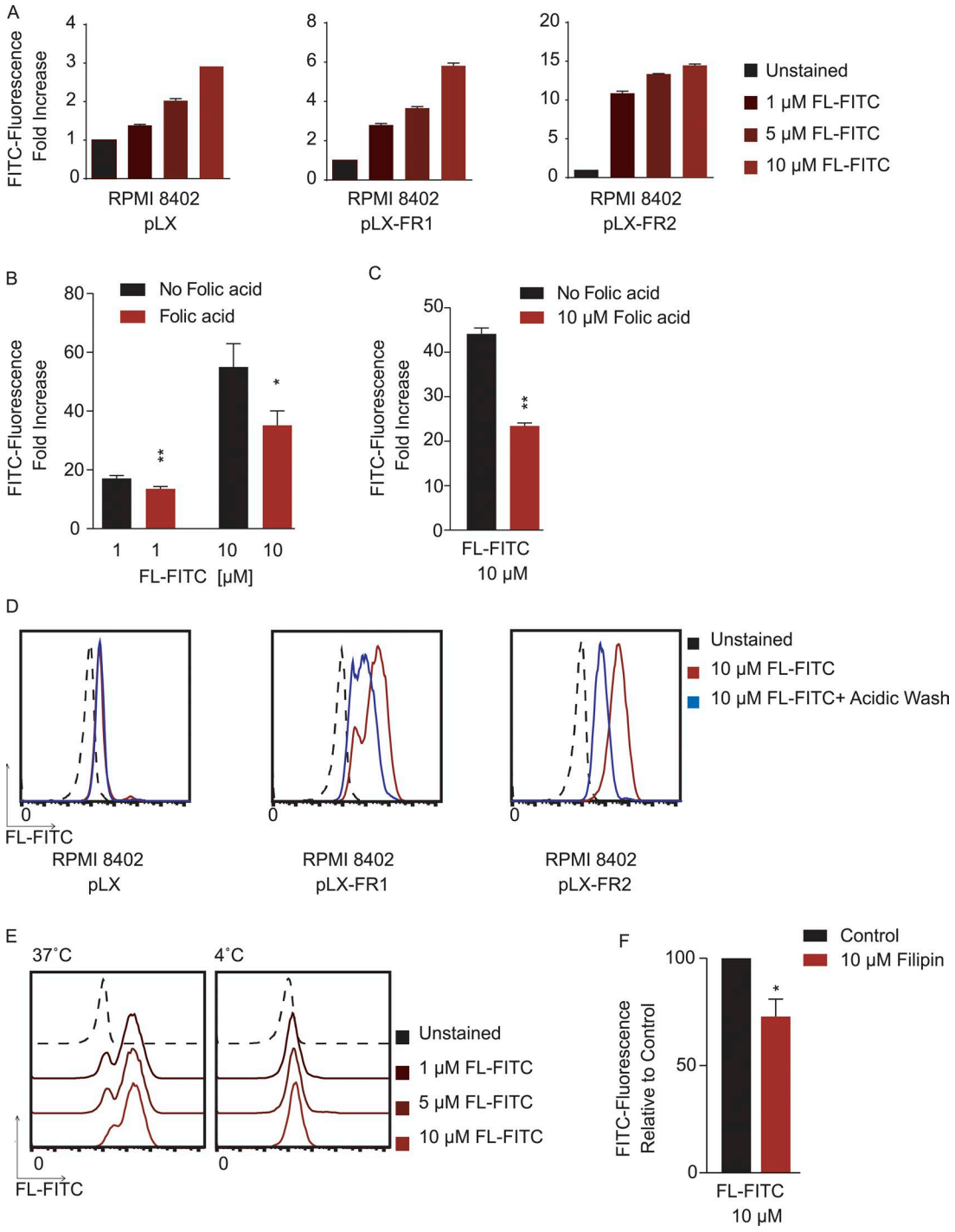

Figure 3. **FL-FITC uptake is folate receptor–dependent in T-ALL by endocytosis. (A)** FITC fluorescence fold increase upon treatment with indicated concentrations of FL-FITC in T-ALL cells overexpressing FR isoforms. Fluorescence signal is depicted as mean fluorescence intensity relative to untreated control. Errors bars denote the mean ± SD of two replicates. **(B)** FITC fluorescence fold increase upon treatment with indicated concentrations of FL-FITC in T-ALL cells (ALL/SIL) cultured in the presence (red) or absence (black) of FA. Fluorescence is expressed as relative activity compared with the untreated control. Error bars denote the mean of FITC fluorescence intensity ± SD of three replicates. Statistical significance for all sample pairs in the experiment (*, $P \leq 0.05$; **, $P \leq 0.01$) was determined by one-way ANOVA using Bonferroni's correction for multiple comparison testing. **(C)** FITC fluorescence fold increase in T-ALL cells (ALL/SIL) cultured in the absence of FA and 10 μM FL-FITC or 10 μM FL-FITC and 10 μM FA. Fluorescence is expressed as relative activity compared with an untreated control. Error bars denote the mean of fluorescence FITC intensity ± SD of two biological replicates. Statistical significance among groups (**, $P \leq 0.01$) was determined by nonparametric *t* test (Mann–Whitney). **(D)** FL-FITC uptake in T-ALL cells in RPMI 8402 cells and RPMI 8402–overexpressing FR isoforms as measured by flow cytometry. Cells were treated with 10 μM FL-FITC and subsequently subjected to an acidic wash

mal organs (Paulos et al., 2004a), and ∼10–20 min in macrophages in inflamed tissues (Varghese et al., 2014). Thus, to exclude the possibility that FR2 is a target of UPR, we first treated T-ALL cell lines with increasing concentrations of Thap-OH for 24 h. No change in FR2 expression was observed by Western blotting (Fig. 5 A). Similarly, in time course studies (0–48 h), no change in FR2 expression was observed in T-ALL treated with JQ-FT or Thap-OH (Fig. 5 B). This result indicates that FR2 is not affected by Thap-OH at concentrations targeting NOTCH1.

Together, these data demonstrate that Thap-OH preferentially inhibits mutant NOTCH1 receptors while sparing wild-type NOTCH1 and FR2 expression, supporting Thap-OH as a suitable and targeted payload for folate-conjugation.

Targeted delivery of folate-conjugated thapsigargin to T-ALL cells

We next studied the effects of JQ-FT in a panel of T-ALL cell lines that contain activating mutations in the heterodimerization domain of *NOTCH1* and/or protein-stabilizing deletions within the PEST degradation domain. In all T-ALL cell lines studied, JQ-FT impaired cell growth, leading to G1 arrest and rapid induction of apoptosis (Fig. 6, A–D). As expected based on our FL-FITC uptake studies, a greater effect on cell viability was observed in cell lines overexpressing FR1 or FR2 (Fig. 6 E). To demonstrate that JQ-FT enters the cells through an FR-based mechanism, we treated T-ALL in the presence or absence of FA (10 and 100 μM; Paulos et al., 2004a). Cells co-treated with FA are rescued from JQ-FT treatment, whereas no differential response was observed in cells treated with Thap-OH (Fig. 6 F), supporting the mechanism of internalization and subsequent cleavage of JQ-FT through an FR mediated process and consistent with the lack of spontaneous degradation to Thap-OH in culture media conditions (Fig. S4).

As observed with thapsigargin and Thap-OH, treatment of T-ALL cell lines with JQ-FT led to accumulation of full-length NOTCH1 (Fig. 7 A). A decrement of transmembrane NOTCH1 (TM-N1) was confirmed by Western blotting and flow cytometry analysis (Fig. 7, A and B). Loss of ICN1 (Fig. 7 A) caused the suppression of NOTCH1 target genes as measured by RT-PCR (Fig. 7 C). Consistent with a folate receptor–mediated process, FA competition rescued the effects of JQ-FT on transmembrane and activated NOTCH1 as measured by Western blotting and flow cytometry (Fig. 7, D and E). FA did not rescue the effects of Thap-OH on NOTCH1 protein levels (Fig. 7, D and E). To establish whether the effects of JQ-FT on cell viability were caused by impaired NOTCH1 activation, the NOTCH1-dependent T-ALL cell line RPMI 8402 was transduced with MigR1-ICN1, to rescue effects on full-length NOTCH1 processing, versus an empty MigR1 vector control. Exogenous expression of ICN1 attenuated the growth-inhibitory effects of JQ-FT, in keeping with the function of ICN1 downstream of ER processing and surface γ-secretase cleavage in Notch pathway activation (Fig. 7 F).

To begin to assess the translational significance of these findings, we studied leukemia cells from T-ALL patient-derived xenografts (PDXs). JQ-FT treatment inhibited the viability of *NOTCH1*-mutated PDX cells in vitro (Fig. 8 A). In addition, JQ-FT treatment resulted in loss of transmembrane NOTCH1, leading to the depletion of detectable ICN1 (Fig. 8, B and C). In contrast, no effect was observed in PDX T-ALL cells with wild-type *NOTCH1* (Fig. 8 B). Consistent with these results, no transcriptional changes were observed in NOTCH1 target genes in wild-type PDX samples, whereas expression of canonical NOTCH1 target genes, *DTX* and *MYC*, was decreased in the *NOTCH1* mutant samples (Fig. 8 D). These results provide strong support for the mechanistic thesis that mutated NOTCH1 receptors are more sensitive to JQ-FT treatment in human T-ALL, prompting proof-of-concept studies in T-ALL models in vivo.

JQ-FT attenuates NOTCH1-driven T-ALL in vivo

In vitro studies provide valuable mechanistic insights but may not recapitulate tumor microenvironment and metabolic conditions in vivo. Indeed, a significant limitation of research on folate-conjugate drugs is the inconsistency between free folate concentrations (and other middle metabolites) in culture conditions in vitro versus in vivo. High levels of free FA in the serum may block the binding and uptake of JQ-FT in FR2-positive T-ALL, compromising the anti-NOTCH1 leukemia effect observed in vitro. To explore the therapeutic efficacy of JQ-FT in vivo, we studied effects on a syngeneic T-ALL mouse model carrying *NOTCH1* L1601P ΔPEST, a common mutation observed in the human disease. First, leukemia cells obtained from this model were treated with JQ-FT for 24 h in vitro. Consistent with the results observed in cell lines and PDX cells, ex vivo treatment with JQ-FT diminished the proliferation (Fig. 9 A), ICN1 expression (Fig. 9, B and C), and transcription of canonical NOTCH1 targets *Hes1* and *Dtx1* (Fig. 9, D and E).

Although the JQ-FT conjugate has not yet been optimized for pharmacologic properties, we were eager to explore the utility of the compound as an in vivo chemical probe,

with PBS, 50 mM Glycine, pH 4.0 (blue) or no wash (red) to eliminate cell surface-bound fluorescence. Untreated cells (dotted line) were used as a control for autofluorescence. **(E)** Fluorescence intensity increase in T-ALL cells cultured at 37°C or 4°C upon folate-FITC treatment as measured by flow cytometry. Experiments were performed in RPMI 8402–overexpressing FR2 isoforms. **(F)** FITC fluorescence in four T-ALL cell lines treated with 10 μM FL-FITC and pretreated with vehicle (black) or 10 μM filipin (red). Errors bars denote the mean ± SD of four cell lines. Statistical significance for difference in treated versus control samples (*, $P \leq 0.05$) was determined by nonparametric *t* test (Mann–Whitney).

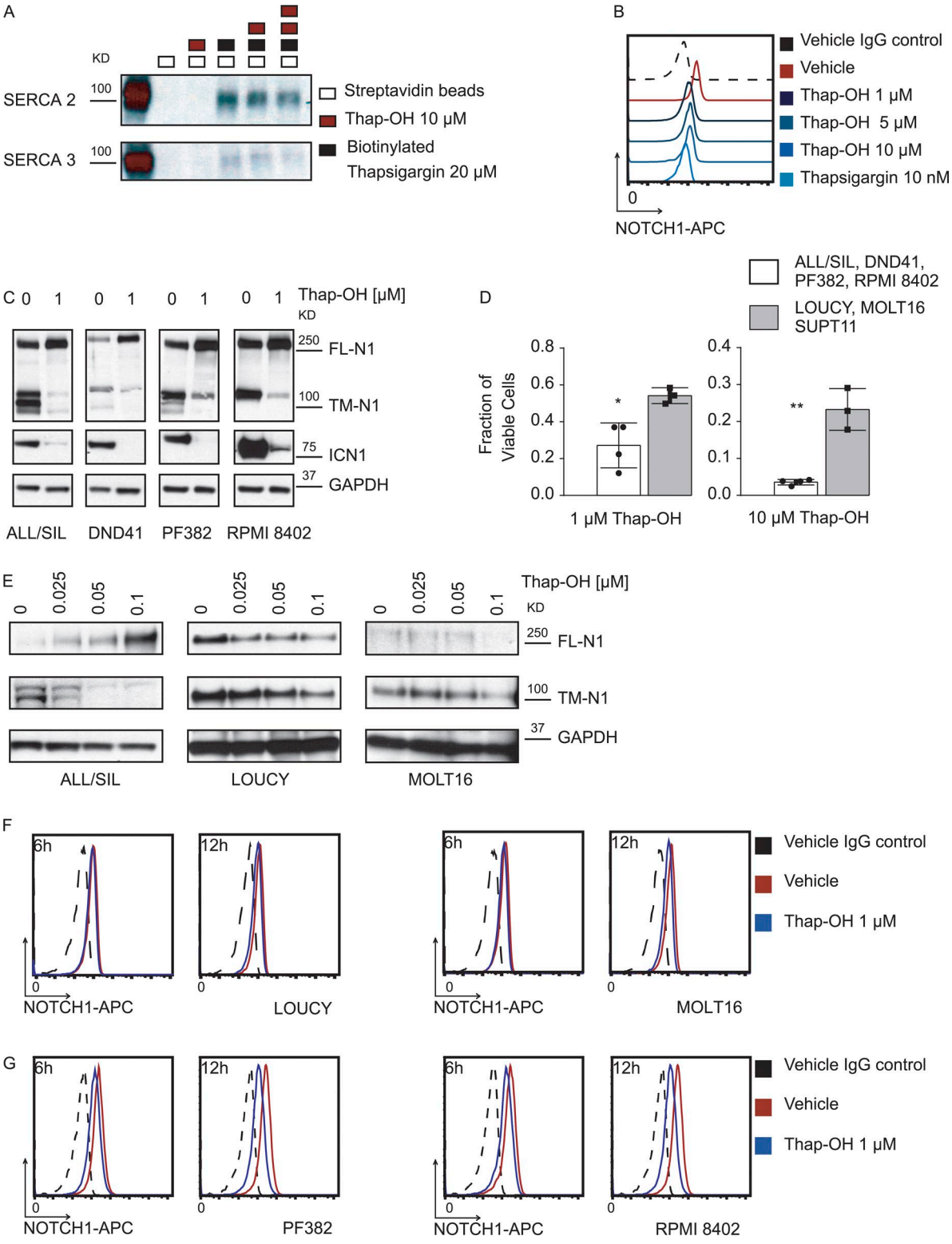

Figure 4. **Thap-OH demonstrates anti-NOTCH1 and antileukemia properties in T-ALL in vitro. (A)** Effect of Thap-OH on SERCA binding. Lysates from T-ALL cells (ALL/SIL) were cotreated with the indicated concentrations of biotinylated thapsigargin or Thap-OH for 6 h and subjected to streptavidin pull-down for 24 h. The immunoblot was stained with SERCA2 and SERCA3 antibodies. **(B)** Effect of 24 h of Thap-OH treatment on NOTCH1 cell-surface staining as assessed by flow cytometry. **(C)** Effect of Thap-OH treatment for 24 h on NOTCH1 (N1) processing and activation in T-ALL cell lines all with heterodimerization mutations (DND41 and ALL/SIL (L1594PΔPEST), PF382 (L1575PΔPEST), and RPMI 8402 (ins1584PVELMPPE). The blot was stained with an

while assessing putative tolerability of folate-conjugated thapsigargin. We first established the feasibility of administering JQ-FT (60 mg/kg per day) in mice, administered by daily i.p. injection. Notably, this tolerated dose is 150-fold improved over our prior established maximum tolerated dose of unconjugated thapsigargin (Roti et al., 2013). Next, we performed pharmacokinetics and tissue distribution of JQ-FT at 60 mg/kg per day in male CD1 mice, which revealed that JQ-FT exhibits broad biodistribution, a low basal rate of hydrolysis to the active thapsigargin, and excellent pharmacologic stability. After a single i.p. injection, JQ-FT achieved a maximum serum concentration of 1,272 ng/ml in bone marrow, 67,952 ng/ml in liver, 2,244 ng/ml in plasma, and 6,416 ng/ml in spleen, with a basal rate of hydrolysis to the active thapsigargin (ratio JQ-FT/Thap-OH; Fig. 9 F). Because these concentrations reached an active concentration range as established in vitro (1–10 μM), we initiated treatment studies of JQ-FT (60 mg/kg i.p. daily) in mice with established T-ALL. After 5 d of treatment, a decrease in tumor growth was observed, confirmed pathologically by a decrease in leukemic infiltration in spleen and liver (Fig. 9 G) and clinically by a reduction in spleen weight (Fig. 9 H). Bone marrow infiltration by T-ALL, the primary site of human disease, was markedly inhibited by JQ-FT, as confirmed by flow cytometric analysis for GFP^+ leukemia cells (Fig. 9 I). Pharmacodynamic modulation of the Notch pathway was importantly validated by measurement of reduced ICN1 expression in T-ALL cells from JQ-FT–treated animals, compared with vehicle-treated controls (Fig. 9, J and K).

DISCUSSION

In the last decade, *NOTCH1* has been identified as one of the most frequently mutated genes across all cancers (Lawrence et al., 2014). In hematologic malignancies, activating *NOTCH1* mutations are observed in chronic lymphocytic leukemia (CLL; Di Ianni et al., 2009; Puente et al., 2011) and mantle cell lymphoma (Kridel et al., 2012) and at an exceptionally high rate in T-ALL (Weng et al., 2004), where *NOTCH1* mutations represent the most common actionable genetic abnormality. Targeted NOTCH1 therapies, such as γ-secretase inhibitors and receptor-blocking antibodies, have entered early-stage clinical trials. However, these modalities have the liability of inhibiting normal NOTCH1 and NOTCH2. In addition to the known potential for gut toxicity (van Es et al., 2005; Deangelo and Silverman, 2006), there is also a significant concern for secondary malignancies, as Notch receptors are established context-specific tumor suppressor genes (Dotto, 2008; Lobry et al., 2011). Thus, the development of tumor-directed inhibitors with selective activity against mutated proteins is highly desirable.

Although inhibition of SERCA proteins to selectively target mutated NOTCH1 with free thapsigargin is promising, thapsigargin is poorly tolerated. Here, we provide a solution involving folate conjugation. We recognize efforts from other groups to create thapsigargin derivatives (Hua et al., 1995; Procida et al., 1998), some of which have been advanced to tumor models (Christensen et al., 2009). In one derivative, mipsagargin (G202; Doan et al., 2015), thapsigargin is conjugated to a peptidyl substrate of the proteolytic enzyme prostate-specific membrane antigen for localized delivery. A phase I clinical study has demonstrated the safety and tolerability of G202 in patients with advanced cancer (Doan et al., 2015). Recognizing the limitations of peptide delivery mechanisms, we have here pursued an all-chemical strategy.

Direct FR targeting has been used in therapeutics for FR overexpressed cancers via the development of anti-FR antibodies in ovarian and lung cancer (Armstrong et al., 2013; Thomas et al., 2013). For example, MORAb-003, farletuzumab, is a humanized antibody targeting FR1 with efficacy demonstrated in preclinical xenograft models of ovarian cancer (Armstrong et al., 2013). Lynn et al. (2015) reported the development of T cells expressing a chimeric antigen receptor (CAR) specific for human FR2 (m909). M909 CAR T demonstrated activity against human AML cell lines in vitro and prevented AML tumor growth in vivo (Lynn et al., 2015). Interestingly, m909 CARs do not inhibit healthy $CD34^+$ hematopoietic stem cells further supporting the development of a FR-targeting approach in leukemia (Lynn et al., 2015). A second approach uses the high affinity of FA to FR to deliver a folate-conjugated chemotherapeutic agent. An example is the development of vintafolide, a water-soluble derivative of FA and the vinca alkaloid desacetylvinblastine hydrazide (Vergote and Leamon, 2015). In preclinical studies, vintafolide has been shown to bind to FR1-positive tumors and exert direct FR anticancer activity (Reddy et al., 2007). A subsequent phase II clinical trial demonstrated that the combination of vintafolide and liposomal doxorubicin significantly improved the median progression-free survival in women with platinum-resistant

antibody against the C terminus of NOTCH1 that recognizes both the furin-processed NOTCH1 transmembrane subunit (TM) and the unprocessed NOTCH1 precursor (FL). The immunoblot was also stained with anti-ICN1 antibody (Val1744) and GAPDH as a loading control. **(D)** Effect of Thap-OH treatment on cell viability after 72 h of treatment in *NOTCH1* mutated T-ALL cells (ALL/SIL, DND41, PF382, RPMI 8402) or wild type (LOUCY, MOLT16, SUPT11). Statistical significance for mutated versus wild type (*, $P \leq 0.05$; **, $P \leq 0.01$) was determined by one-way ANOVA with Bonferroni's correction for multiple comparison testing. Error bars denote the mean ± SD of four NOTCH1 mutated T-ALL cell lines (ALL/SIL, DND41, PF382, and RPMI 8402) and three NOTCH1 wild-type T-ALL cell lines (LOUCY, MOLT16, and SUPT11). **(E)** Effect of Thap-OH treatment (24 h) on processing of NOTCH1 mutant (ALL/SIL) or wild-type (LOUCY, MOLT16) NOTCH1 receptors. NOTCH1 (N1) was detected with an antibody against the C terminus of NOTCH1 that recognizes the furin-processed NOTCH1 transmembrane subunit (TM) and the unprocessed NOTCH1 precursor (FL). GAPDH was used as loading control. **(F)** Effect of Thap-OH treatment (6 and 12 h) on wild-type NOTCH1 (Loucy, MOLT16) cell surface staining as assessed by flow cytometry. **(G)** Effect of Thap-OH treatment (6 and 12 h) on mutated NOTCH1 (PF382, RPMI 8402) cell surface staining as assessed by flow cytometry.

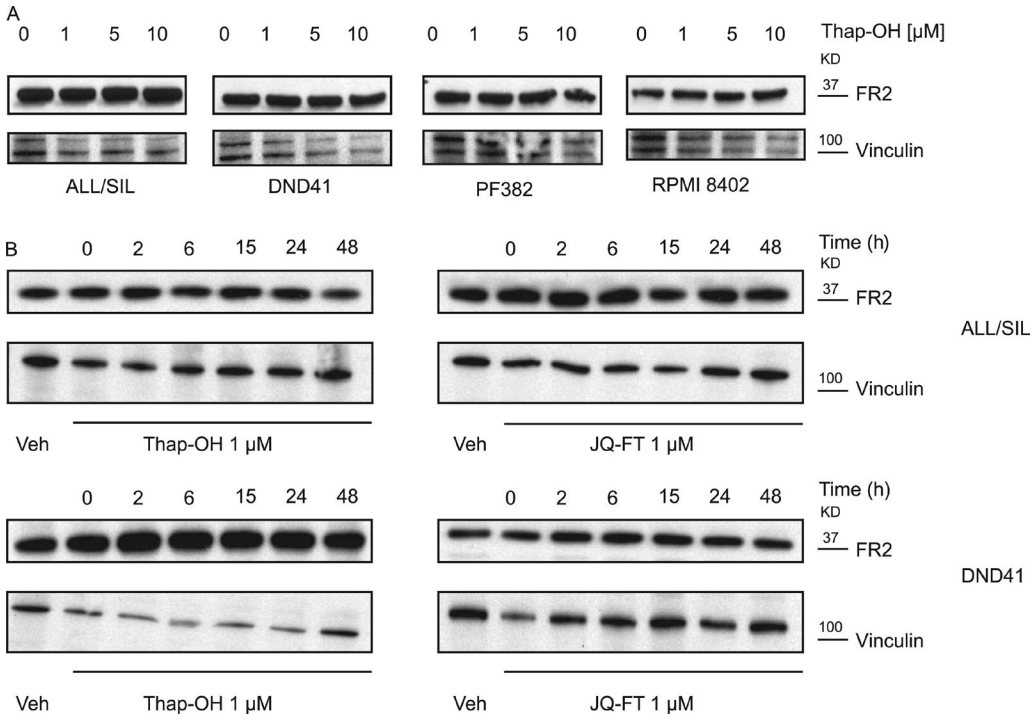

Figure 5. **Thapsigargin derivatives have no effect on FR2 expression. (A)** Effect of Thap-OH treatment (24 h) on FR2 in T-ALL cells. Immunoblot was stained with an antibody against FR2. Vinculin was used as a loading control. **(B)** Time course effect of Thap-OH or JQ-FT treatment on FR2 in T-ALL cells. Immunoblot was stained with an antibody against FR2. Vinculin was used as a loading control.

ovarian cancer (Vergote and Leamon, 2015). However, recent studies of vintafolide failed to confirm these results in a phase III trial (PROCEED trial EC-FV-06), and the study was suspended. Importantly, the decision was not based on safety concerns for the patients enrolled in the trial. Although these results are disappointing, they were partially predictable based on previous experiences that demonstrated the modest clinical benefit in patients treated with vinca alkaloids in this subset of highly aggressive tumors (Rothenberg et al., 2004; Katsaros et al., 2005; Herzog et al., 2008). We hypothesize that simply tagging a generic chemotherapeutic agent to FA may not be sufficient: it is likely important that the selected agent independently demonstrate a robust tumor-specific inhibitory effect. To this end, the folic conjugation serves to simply improve the agent's delivery, uptake, and specificity.

In this study, we have proposed, for the first time, the use of small-molecule folate-mediated delivery of thapsigargin to enable selective and target-specific drug delivery to T-ALL cells. The inhibitor, thapsigargin, was connected to FA with a cleavable bond and was transferred into the cell after binding to FR on the cell surface. The expression of FR in T-ALL enabled the selective recognition of the designed molecule, JQ-FT, by cancer cells. The cleavable bond feature of the molecule facilitated direct delivery of the inhibitory motif to the target (SERCA) and subsequently blocked mutant NOTCH1 maturation. This strategy avoided complicated manufacturing processes, such as drug–antibody conjugation, but still allowed selective delivery to the cancer cell. Indeed, the dose of JQ-FT tolerated in mice was >150-fold that of thapsigargin, supporting the more selective uptake of the derivatized product. Importantly, in our in vivo experiments, mice were not restricted to a low folate chow to demonstrate FR-mediated antitumor effect in vivo. Such a strategy had been reported in previously published preclinical studies testing folate-drug conjugates (Leamon et al., 2008). JQ-FT treatment with a low folate diet is expected to have even greater efficacy in vivo. Although we provide here a prototype molecule, JQ-FT is not yet a drug molecule. Additional medicinal chemistry will be needed to optimize the compound for clinical translation, including optimization of the probe, delivery strategy, and schedule of administration. For example, the potency of the molecule will likely require improvement, potentially by the addition of a cleavable spacer between FA and thapsigargin, avoiding the need for Thap-OH, which is less potent than thapsigargin.

In conclusion, the described approach enhanced the therapeutic window of thapsigargin as a NOTCH1 inhibitor providing dual selectivity: leukemia over normal cells and NOTCH1 mutated over wild-type receptors. Given the important role of mutations in *NOTCH1* in many cancers, JQ-FT offers a potential strategy in treating other tumors with *NOTCH1* mutations, such as CLL and non–small cell lung cancer. Furthermore, our study demonstrated both in vitro and in vivo that the folate-assisted, pathway-specific drug delivery

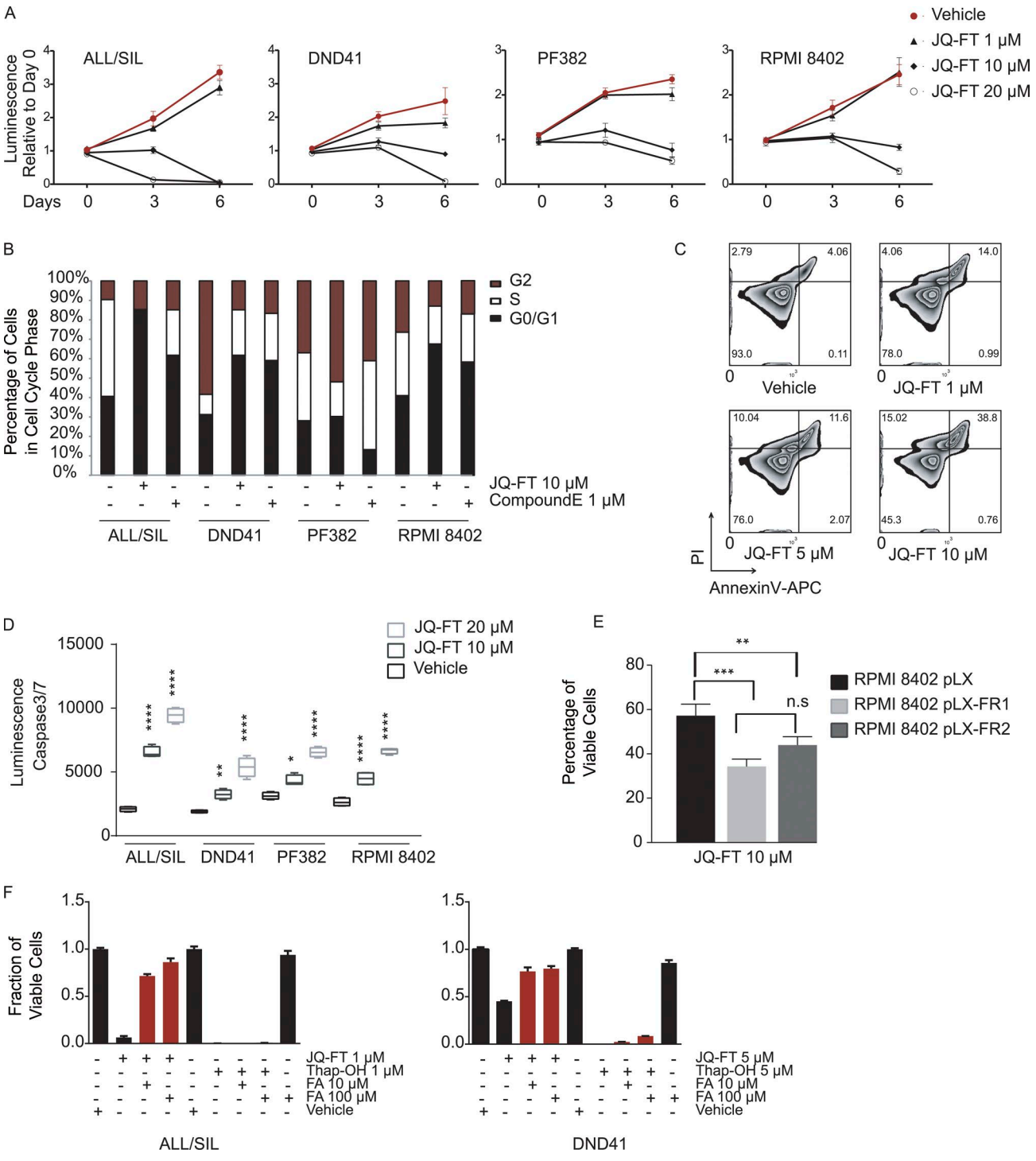

Figure 6. **JQ-FT demonstrates antileukemia properties in T-ALL in vitro. (A)** Effect of JQ-FT treatment on cell growth. Errors bars denote mean ± SD of four replicates. **(B)** Effect of JQ-FT treatment (6 d) on cell cycle of T-ALL cell lines as assessed by measurement of DNA content on the viable fraction of cells. **(C)** Effect of JQ-FT treatment on induction of apoptosis. Annexin V/propidium iodide staining of T-ALL (ALL/SIL) cells after 72 h of treatment with increasing concentrations of JQ-FT. **(D)** Effect of JQ-FT treatment on apoptosis induction as assessed by the luminescence caspase 3/7 assay. Errors bars denote mean ± SD of four replicates. Statistical significance among groups for treated versus vehicle (DMSO; *, $P \leq 0.05$; **, $P \leq 0.01$; ****, $P \leq 0.0001$) was determined by one-way ANOVA using Bonferroni's correction for multiple comparison testing. **(E)** Effect of JQ-FT on the growth of *FOLR1* or *FOLR2*-transduced RPMI 8402 cells. Normalized data are plotted relative to vehicle. Error bars indicate mean ± SD of four replicates. Statistical significance among treated samples with JQ-FT 10 μM (**, $P \leq 0.01$; ***, $P \leq 0.001$) was determined by one-way ANOVA with Bonferroni's correction for multiple comparison testing. **(F)** Effect of JQ-FT and Thap-OH treatment (72 h) on cell viability in T-ALL cell lines all with heterodimerization mutations in the presence or absence of excess of FA (10 or 100 μM). Error bars indicate mean ± SD of four replicates.

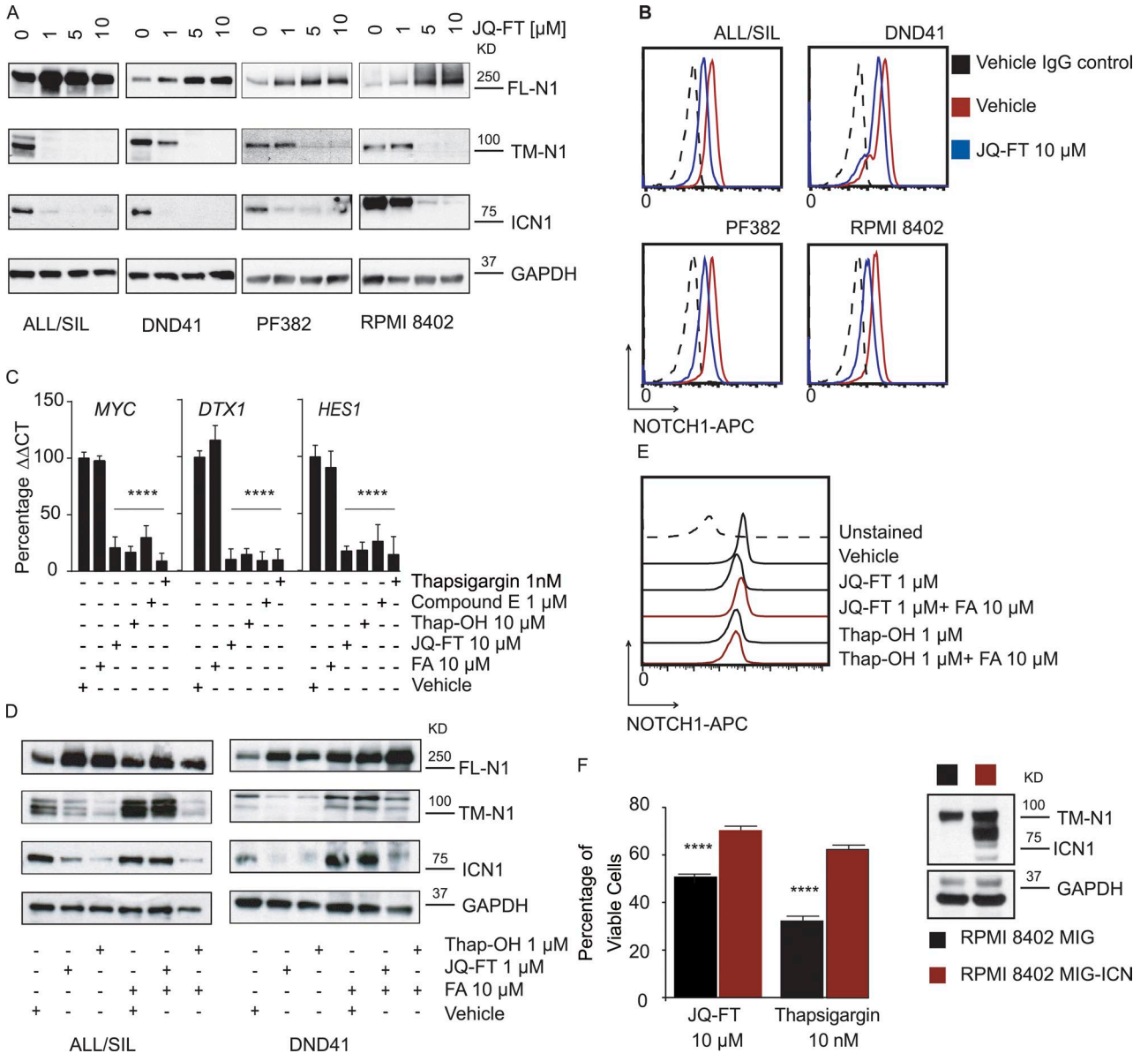

Figure 7. **JQ-FT demonstrates anti-NOTCH1 properties. (A)** Effect of JQ-FT treatment (24 h) on NOTCH1 (N1) processing and activation in T-ALL cell lines all with heterodimerization mutations. The blot was stained with an antibody against the C terminus of NOTCH1 that recognizes both the furin-processed NOTCH1 transmembrane subunit (TM) and the unprocessed NOTCH1 precursor (FL). The immunoblot was also stained with anti-ICN1 antibody. GAPDH was used as a loading control. **(B)** Effect of 24-h JQ-FT treatment on NOTCH1 cell surface staining as assessed by flow cytometry. **(C)** Mean expression of NOTCH1 target genes in T-ALL cells (PF382, RPMI 8402) treated for 24 h with the indicated concentrations of thapsigargin, JQ-FT, Thap-OH, FA, or the γ-secretase inhibitor compound E was determined by quantitative RT-PCR. Error bars indicate the mean ± SD of four replicates. Data were analyzed using the ΔΔCT method and plotted as a percentage relative to the control gene *RPL13A*. Statistical significance among groups for treated versus vehicle (DMSO) samples (****, $P \leq 0.0001$) was determined by one-way ANOVA with Bonferroni's correction for multiple comparison testing. **(D)** Effect of JQ-FT and Thap-OH treatment (24 h) on NOTCH1 (N1) processing and activation in T-ALL cell lines all with heterodimerization mutations in the presence or absence of excess of FA (10 μM). The blot was stained with an antibody against the C terminus of NOTCH1 that recognizes both TM and FL. The immunoblot was also stained with anti-ICN1 antibody. GAPDH was used as a loading control. **(E)** Effect of 24 h of JQ-FT and Thap-OH treatment in the presence or absence of excess of FA (10 μM) on NOTCH1 cell-surface staining as assessed by flow cytometry. **(F)** Effect of JQ-FT on the growth of MigR1 or MigR1-ICN1–transduced RPMI 8402 cells. Normalized data are plotted relative to vehicle. Error bars indicate mean ± SD of four replicates. Statistical significance for treated versus vehicle (DMSO; ****, $P \leq 0.0001$) was determined by one-way ANOVA with Bonferroni's correction for multiple comparison testing.

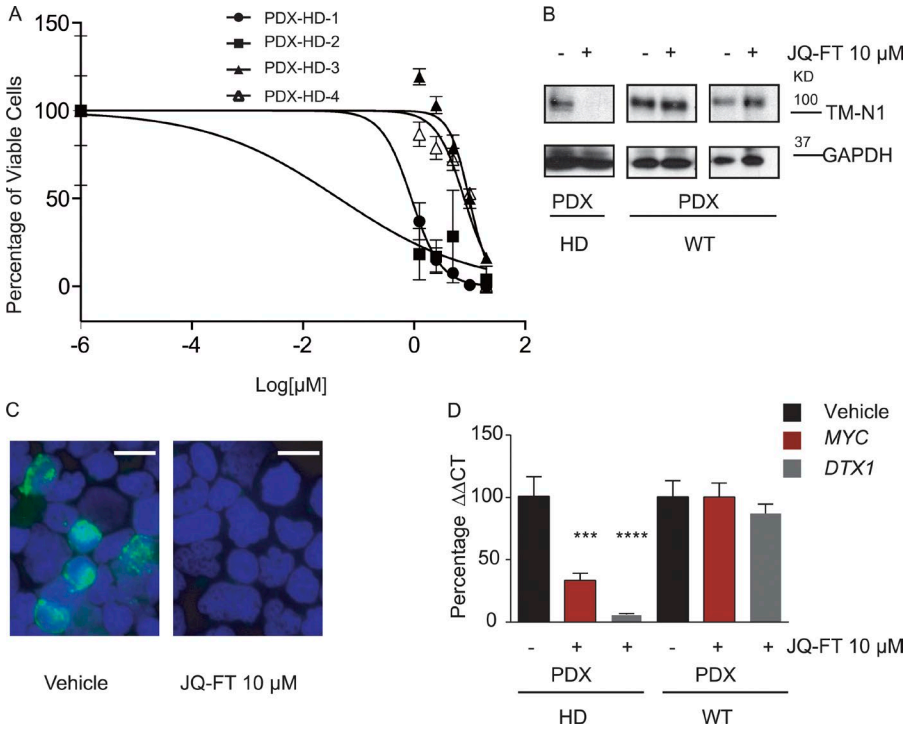

Figure 8. **JQ-FT demonstrates anti-NOTCH1 properties in PDX cells. (A)** Effect of JQ-FT treatment on cell viability in PDX T-ALL cells ex vivo. Errors bars denote mean ± SD of four replicates. **(B)** Effect of JQ-FT treatment (24 h) on NOTCH1 processing in PDX cells in vitro. The blot was stained with an antibody against the C terminus of NOTCH1 (N1) that recognizes both the furin-processed NOTCH1 transmembrane subunit (TM) and the unprocessed NOTCH1 precursor (FL). GAPDH was used as a loading control. **(C)** Immunofluorescence analysis of JQ-FT treatment (24 h) on NOTCH1 activation in permeabilized PDX cells in vitro. Cells were probed with an anti-NOTCH1 antibody (green), and nuclei were counterstained with DAPI. Images were acquired at 60× magnification. Bars, 10 μm. **(D)** Expression of indicated NOTCH1 target genes in T-ALL PDX cells treated with JQ-FT for 24 h was determined by quantitative RT-PCR. Error bars indicate the mean ± SD of four replicates. Data were analyzed using the ΔΔCT method and plotted as a percentage relative to the control gene *RPL13A*. Statistical significance (***, $P \leq 0.001$; ****, $P \leq 0.0001$) for treated versus vehicle (DMSO) was determined by one-way ANOVA with Bonferroni's correction for multiple comparison testing.

strategy could be an efficient method to solve a common drug delivery problem in the present era of targeted cancer therapy.

MATERIALS AND METHODS

Cell culture

Human cell lines MOLT16, LOUCY, DND41, and HPB-ALL were purchased from Leibniz-Institut DSMZ-German collection of microorganisms and cell cultures and ATCC; identity of ALL/SIL, KOPTK1, PF382, SUPT11, and RPMI 8402 was confirmed by PCR sequencing for known *NOTCH1* mutations and short tandem repeat loci profiling. Cells were cultured in RPMI 1640 (Cellgro) with 10% FBS (Sigma-Aldrich) and 1% penicillin-streptomycin and incubated at 37°C with 5% CO_2. Primary patient cells were collected from peripheral blood or bone marrow aspirates, after obtaining informed consent under Dana-Farber Cancer Institute Internal Review Board (DFCI IRB)–approved protocols. Patient-derived xenografted cells were provided by David Weinstock at the Dana-Farber Cancer Institute under DFCI IRB–approved protocols. Cells were cultured short-term in RPMI 1640 with 10% FBS and 1% penicillin-streptomycin and incubated at 37°C with 5% CO_2 supplemented with IL-2 (0.1 ng/ml) and IL-7 (0.1 ng/ml; Peprotec).

Isolation of T cells from human blood

Separation of T cells from PBMCs was obtained by depletion of non-T cells using the Pan T Cell Isolation kit (130–096-535), an LS Column, and a MidiMACS Separator (Miltenyi Biotec). PBMCs were first isolated from human healthy donors by using a density gradient medium (Ficoll-Paque PLUS; GE Healthcare). All primary human samples were de-identified and obtained after informed consent through DFCI IRB–approved protocol 04-430.

Isolated PBMCs were immediately incubated with a pan-T cell microbeads cocktail for 15 min at 4°C and separated using a magnetic column according to the manufacturer's protocol. RPMI medium was used for the incubation of isolated T cells. Cells were labeled with CD3-FITC (Beckman Coulter) and analyzed by flow cytometry with an Accuri C6 (BD).

Viral transduction

Oligonucleotides encoding cDNA-ORF (*FOLR1* and *FOLR2*) were cloned into pLK317 obtained from the Broad Institute of Harvard and MIT. For virus production, 500,000 293T cells plated in 10-cm plates were transfected with 1 μg pLK317 and packaging plasmids according to the FuGENE 6 protocol (Roche Diagnostics). Medium was changed to RPMI 1640 24 h posttransfection, and viral supernatant was harvested and filtered 48 h posttransfection. The virus was concentrated five times using Peg-it virus precipitation solution (System Bioscences). Cells were infected for 2 h at 37°C with 2 ml lentivirus and 8 μg/ml polybrene (Sigma-Aldrich). Cells were selected 48 h later with 1 μg/ml puromycin (Sig-

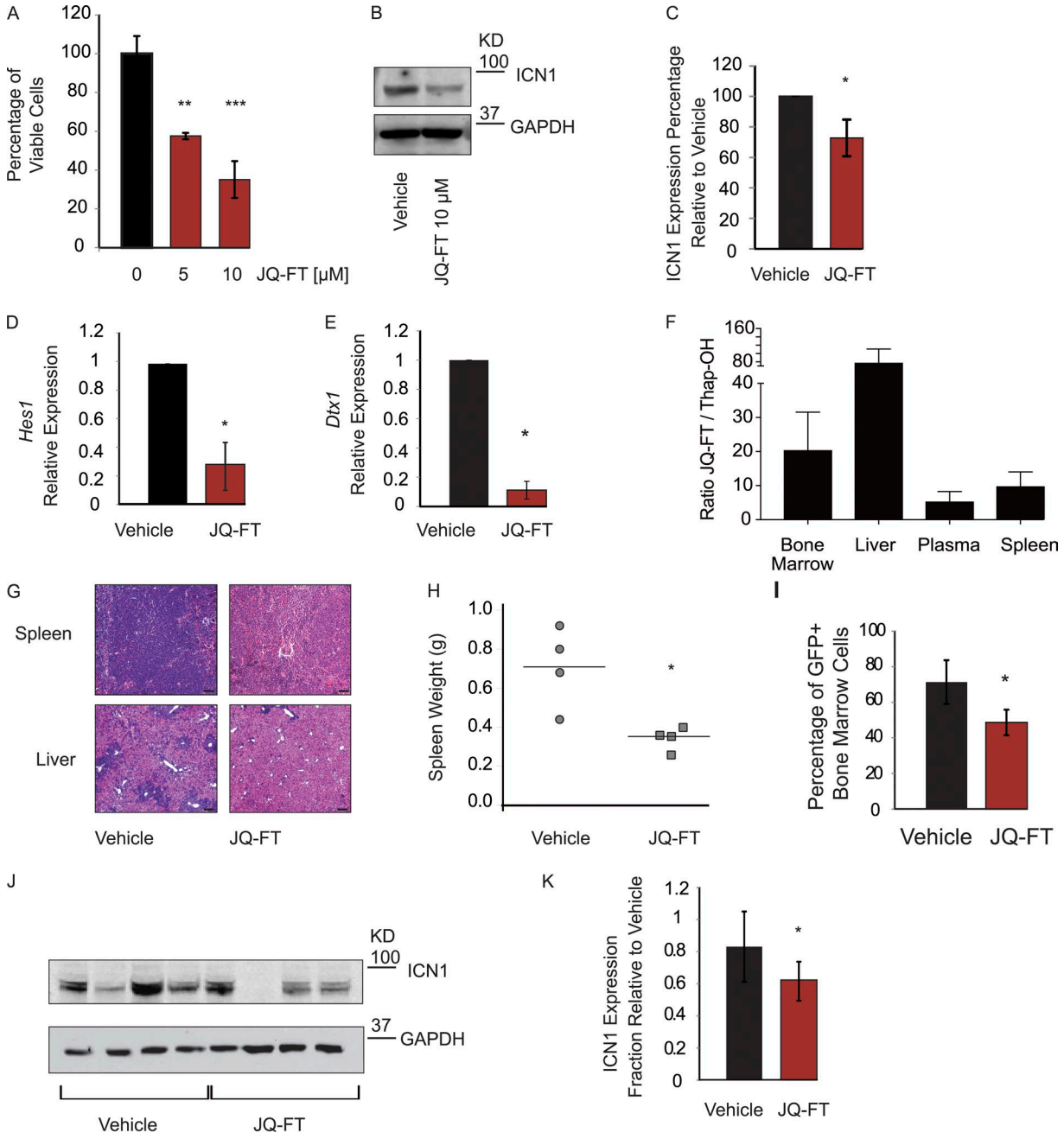

Figure 9. **JQ-FT demonstrates activity in T-ALL mouse model. (A)** Effect of JQ-FT treatment on cell growth (72 h) in murine NOTCH1 L1601P ΔPEST–expressing leukemia cells. Viability data are represented as percentage relative to vehicle treatment and errors bars denote mean ± SD of three replicates. Statistical significance of treated versus vehicle (DMSO) samples (**, $P \leq 0.01$; ***, $P \leq 0.001$) was determined by one-way ANOVA with Bonferroni's correction for multiple comparison testing. **(B)** Effect of JQ-FT on ICN1 levels in murine NOTCH1 L1601P ΔPEST–expressing leukemia cells. The immunoblot contains cell lysates stained with anti-ICN1 antibody (Val1744) after treatment with 10 μM JQ-FT for 24 h in vitro. GAPDH was used as a loading control. **(C)** ICN1 loss was quantified, and the bar graph corresponds to the results of the quantification of three independent experiments. Statistical significance of treated versus vehicle (DMSO) samples (*, $P \leq 0.05$) was determined by Student's *t* test. Error bars denote the mean ± SD of two indipendent experiments. **(D and E)** Expression of indicated NOTCH1 target genes *Hes1* (D) *and Dtx1* (E) in murine NOTCH1 L1601P ΔPEST–expressing leukemia cells treated with 10 μM JQ-FT for 24 h was determined by quantitative RT-PCR. Error bars indicate the mean ± SD of three replicates. Data were analyzed using the ΔΔCT method and plotted as a percentage relative to the control gene *Gapdh*. Statistical significance for treated versus vehicle (DMSO; *, $P \leq 0.05$) was determined by Student's *t* test. **(F)** Pharmacokinetic ratio analysis of JQ-FT to Thap-OH. Quantification expressed as hydrolysis ratio of JQ-FT/Thap-OH in bone marrow, liver, plasma, and spleen after i.p. injection of 60 mg/Kg JQ-FT at 50 min. Error bars indicate mean ± SD of three replicates (three mice/time point). **(G)** Histological analysis of the spleen and the liver in a NOTCH1 L1601P ΔPEST murine model treated with JQ-FT 60 mg/kg or vehicle for 5 d. The spleen and the liver of all mice were examined; representative results for one control animal and one JQ-FT–treated animal are shown. Formalin-fixed, paraffin-embedded

ma-Aldrich). Viral supernatant production and retroviral infections were performed as previously described for MigR1 retroviral vectors (Aster et al., 2000). Transduction efficiency for MigR1 was monitored by assessing GFP expression with a FACScan flow cytometer (BD). After viral infection, GFP-positive cells were sorted by flow cytometry with a FACSAria II (BD) and cultured under compound E (0.5 μM) negative selection for 10 d. Experiments were conducted 3 or more days after removal of compound E.

Cell growth, apoptosis, and DNA content assays

Cell growth was assessed using the Cell-TiterGlo ATP-based assay (Promega). Luminescence was measured using a Fluostar Omega instrument (BMG-Labtech). Apoptosis was measured using a Caspase-Glo 3/7 assay (Promega), or by annexin V and propidium iodide staining by flow cytometry (eBioscience). Cellular DNA content was assessed by staining with propidium iodide (50 g/ml). Cells were analyzed by flow cytometry with a FACScan flow cytometer (BD) and FlowJo V10 (Tree Star) analytical software. At least 20,000 events were acquired, and all determinations were replicated at least twice.

To assess cell viability upon JQ-FT treatment, in vitro murine leukemia cells expressing *NOTCH1* L1601P ΔPEST were cultured in Optimem medium supplemented with 10% FBS, 1% penicillin/streptomycin, and murine IL-7 (10 ng/ml) on a feeder layer of OP9 stromal cells. Viability was examined using the cell viability kit with counting beads from BD, gating out dead cells and particles. Results were analyzed using FlowJo software.

Real-time RT-PCR

Primers and probes for real-time RT-PCR were obtained from Applied Biosystems (*GAPDH* #402869, *RPL13A* #Hs01926559_g1, *MYC* #Hs00153401_m1, *HES1* #Hs00172878_m1, *DTX1* #Hs00269995_m1, *FOLR1* #Hs01124177_m1, *FOLR2* #Hs01044732_g1). The data were analyzed using the ΔΔCT method and plotted as percentage of transcript compared with vehicle.

Immunodetection of NOTCH and folate receptors

Western blots were stained with antibodies specific for γ-secretase–cleaved NOTCH1 (Val1744; #4147 or #2421; Cell Signaling Technology), the intracellular transcriptional activation domain of NOTCH1 (Hasserjian et al., 1996), or the C terminus of NOTCH1 (#SC-6014 [C-20]; Santa Cruz Biotechnology). Control stains were performed with antibodies specific for actin (#ACTN05; Thermo Fisher Scientific), vinculin (#2907; Abcam), or GAPDH (#137179; Santa Cruz Biotechnology). Blots were developed with anti-rabbit HRP (#NA9340V; Amersham) or anti-mouse-HRP (#NA9310V; Amersham).

Expression of FR1 and FR2 was determined using isoform-specific antibodies (#MAB5646, R&D Systems; #103988, Abcam). Immunofluorescence staining was performed on permeabilized cells using a murine monoclonal antibody against NOTCH1 (3294, Abcam), and species-specific secondary antibodies linked to Alexa Fluor 488. Slides were mounted with Prolong Gold anti-fade reagents and counterstained with DAPI (Invitrogen). Images were acquired using a Zeiss LSM510 confocal microscope at 100× power. Cell surface NOTCH1 was evaluated by staining nonpermeabilized cells with monoclonal anti-human NOTCH1 antibody (#FAB5317P; R&D Systems) as previously described (Roti et al., 2013).

Measurement of FL-FITC and FL-TAMRA

The fluorescent folate analogues folate-FITC (FL-FITC) and folate-TAMRA (FL-TAMRA) were synthesized as described in the Supplemental Material. T-ALL cells were grown in the presence or absence of FL-FITC, and after treatment, cells were washed in cold PBS containing 2 mmol/L EDTA. Background fluorescence on the cell surface due to nonspecific FA fluorescence was determined in each experiment by incubating cells with free FA. For internalization studies, T-ALL cells were incubated for 6 h at 37°C and subsequently either washed as described above or subjected to a short acidic cold wash with PBS, 50 mM glycine pH 4.0 to eliminate cell surface-bound fluorescence. Fluorescent signal was assessed using flow cytometry with an Accuri C6 (BD). A minimum of 10,000 events was collected for each biological sample. TAMRA fluorescence was assessed using a Fluostar Omega instrument (BMG-labtech) with excitation set at 541 wavelength and emission at 568 nM.

tissue sections were stained with hematoxylin and eosin. Growth suppression of leukemia cells (dark purple) was observed in JQ-FT–treated animals. Bars, 10 μm. **(H)** Effect of JQ-FT on T-ALL growth in a NOTCH1 L1601P ΔPEST murine model. Antileukemic activity of JQ-FT was assessed by measuring spleen weight after 5 d of treatment with JQ-FT (60 mg/kg i.p.) or vehicle (65% D5W + 30% PEG-400 + 5% Tween-80 only). The chart shows spleen weight for each animal (each dot), and the horizontal bar represents the mean of the four animals per group. Statistical significance for treated versus vehicle (*, $P \leq 0.05$) was determined by nonparametric *t* test (Mann–Whitney). **(I)** Antileukemic activity of JQ-FT on bone marrow NOTCH1 L1601P ΔPEST GFP-positive leukemia cells after 5 d of treatment with JQ-FT (60 mg/kg i.p.) or vehicle (65% D5W + 30% PEG-400 + 5% Tween-80 only). Error bars indicate mean ± SD of four replicates (of the four animals of each group). Statistical significance for treated versus vehicle (*, $P \leq 0.05$) was determined by nonparametric *t* test (Mann–Whitney). **(J)** Effect of JQ-FT on Notch activation in a NOTCH1 L1601P ΔPEST murine model. The immunoblot contains splenic cell lysates stained with anti-ICN1 antibody (Val1744) after treatment with 60 mg/kg JQ-FT for 5 d. GAPDH was used as a loading control. **(K)** ICN1 loss was quantified, and bar graph corresponds to the results of the quantification. Statistical significance for treated versus vehicle (*, $P \leq 0.05$) was determined by Student's *t* test. Error bars denote the mean ± SD of the four samples loaded in the immunoblot depicted in J.

T-ALL in vivo experiments

Pharmacokinetics and biodistribution studies were performed at ChemPartner in Shanghai, China. In brief, three male CD1 mice were i.p. injected per time point with 60 mg/kg JQ-FT dissolved in 65% D5W + 30% PEG-400 + 5% Tween-80 and sampling of plasma, bone marrow, liver and spleen were collected at multiple time points. JQ-FT concentration was assessed by liquid chromatography (LC)/tandem mass spectrometry (MS-MS) method and pharmacokinetics parameters (T_{max}, C_{max}, $T_{1/2}$, AUC, etc.) calculated with WinNonlin V 6.2 statistics software (Pharsight Corporation) using a noncompartmental model.

Animals for efficacy studies were maintained in specific pathogen–free facilities at the Irving Cancer Research Center at Columbia University Medical Campus. Animal procedures were approved by the Columbia University IACUC. To generate NOTCH1-induced T-ALL tumors in mice, retroviral transduction of bone marrow cells enriched in lineage negative cells (#130-090-858; Miltenyi) according to the manufacturer's guidelines was performed with an activated form of the *NOTCH1* oncogene (*NOTCH1* L1601P ΔPEST). Cells were then transplanted via intravenous injection into lethally irradiated recipients. To evaluate the activity of the JQ-FT compound in vivo, leukemia cells expressing the mutant form of *NOTCH1* and GFP were reinjected into sub-lethally irradiated secondary recipients (4 Gy) 6–8 wk old C57BL6 female mice (Taconic Farms). Secondary tumor development was monitored via GFP detection in peripheral blood. Once disease was established, animals with homogeneous tumor burden were divided into two treatment groups of four mice each: vehicle (65% D5W + 30% PEG-400 + 5% Tween-80 only) or 60 mg/kg of JQ-FT. Animals were treated with either vehicle or intraperitoneal injection of compound at 60 mg/kg daily for 5 d. Antileukemic activity of JQ-FT was assessed by measuring spleen weight and percentage of GFP positive (GFP^+) leukemia cells in the bone marrow.

Compound sources

Compounds were obtained from the following sources: compound E (#ALX-270-415-M001, ENZO Life Sciences), filipin (#F9765, Sigma-Aldrich), FA (#F8758, Sigma-Aldrich). Thapsigargin was directly purchased from Adipogene (#AG-CN2-0003). The structure and purity of compounds were further confirmed by nuclear magnetic resistance (NMR) and liquid chromatography and mass spectrometry (LCMS).

Synthesis of small molecule inhibitors and probes

Reactions were run as described in the individual procedures using standard double manifold and syringe techniques; glassware was dried by baking in an oven at 130°C for 12 h before use. Solvents for reactions were purchased anhydrous from Sigma-Aldrich and used as received. HPLC grade solvents were used for aqueous work ups and chromatography. Reagents were used as received. Reactions were monitored by thin-layer chromatography using EMD silica gel 60 F254 (250-micrometer) glass-backed plates (visualized by UV fluorescence quenching and staining with $KMnO_4$) and by LC-MS using a Waters Acquity BEH C18 2 × 50-mm 1.7-μm particle column (50°C) eluting at 1 ml/min with H_2O/acetonitrile [0.2% vol/vol added formic acid; 95:5(0min)→5:95(3.60min)] using alternating positive/negative electrospray ionization (125–1000 amu) and UV detection (210–350 nm). Flash column chromatography was performed using Merck grade 9385 silica gel 60 Å pore size (230–400 mesh; Sigma-Aldrich, St. Louis, MO, USA). Melting points were obtained using a capillary melting point apparatus and are uncorrected. 1H NMR spectra were recorded at 400 MHz on a Bruker spectrometer and are reported in ppm using the residual solvent signal (dimethylsulfoxide-d6 = 2.50 ppm; chloroform-d = 7.27 ppm; methanol-d4 = 3.31 ppm; dichloromethane-d2 = 5.32 ppm) as an internal standard. Data are reported as: {(δ shift), [(s = singlet, d = doublet, dd, doublet of doublets, ddd = doublet of a dd, t = triplet, quin = quintet, sept = septet, br = broad, ap = apparent), (J = coupling constant in Hz) and (integration)]}. Proton-decoupled ^{13}C NMR spectra were recorded at 100 MHz on a Bruker spectrometer (Bruker Daltonics Inc.) and are reported in ppm using the residual solvent signal (chloroform-d = 77.0 ppm; dimethylsulfoxide-d6 = 39.51 ppm; methanol-d4 = 49.15 ppm) as an internal standard. Infrared spectra were recorded using an ATR-FTIR instrument. High-resolution mass spectra were acquired by flow injection on a qTOF Premiere Mass Spectrometer operating in ES+ ionization with resolution ∼15,000.

Synthesis of JQ-FT (Fig. S1). To a solution of thapsigargin (200 mg, 0.31 mmol) in methanol (4 ml), triethylamine (0.5 ml) was added at 23°C. The resulting clear solution was stirred at 23°C for 6 h. The solvent was removed *in vacuo*. The crude reaction was purified directly using column chromatography (MeOH-CH_2Cl_2, 0 to 15% gradient), and produced Thap-OH as white foam (170 mg, 94% yield). MS: m/z $(M+1)^+$: 581.3.

To a solution of Thap-OH (17 mg) in DMSO (1.6 ml) was added FA (27 mg, 0.06 mmol), *N, N'*-dicyclohexylcarbodiimide (DCC, 9.7 mg, 0.077 mmol), and 4-dimethylaminopyridine (DMAP, 3.8 mg, 0.031 mmol). The reaction was stirred at 23°C for 16 h. The reaction mixture was further diluted with methanol and was directly purified by HPLC to afford JQ-FT as yellow powder (13 mg, 45% yield). ^1H NMR (500 MHz, DMSO-d_6) d ppm 0.79–0.89 (m, 5 H), 0.98–1.02 (m, 1 H), 1.11–1.17 (m, 4 H), 1.19–1.33 (m, 19 H), 1.44–1.55 (m, 3 H), 1.64–1.75 (m, 5 H), 1.78–1.82 (m, 8 H), 1.85–1.90 (m, 5 H), 1.95–2.02 (m, 2 H), 2.18–2.35 (m, 6 H), 3.07 (d, J = 11.60 Hz, 1 H), 4.26–4.32 (m, 1 H), 4.35 (br. s., 1 H), 4.45–4.52 (m, 3 H), 5.24–5.27 (m, 1 H), 5.39 (t, J = 3.51 Hz, 1 H), 5.52 (br. s., 1 H), 5.59 (br. s., 1 H), 6.03–6.19 (m, 5 H), 6.55–6.71 (m, 3 H), 7.61 (d, J = 8.85 Hz, 3 H), 8.25 (d, J = 7.63 Hz, 1 H), and 8.60–8.71 (m, 2 H). MS: m/z $(M+1)^+$: 1004.4.

Synthesis of fluorescence FA derivatives (Fig. S2). FA (502.5 mg, 1.14 mmol) and DMAP (692.5 mg, 5.67 mmol) were

suspended in DMSO (5 ml). *N,N′*-diisopropylcarbodiimide (DIC; 350.8 µl, 2.27 mmol) was added to the reaction followed by a solution of SI-1 (204.9 mg, 1.17 mmol) in DMSO (2 ml). The reaction was stirred at room temperature, and an additional 2 ml of DMSO was added to help solubilize the reactants. The reaction was stirred at room temperature overnight. Water was added to the solution, and a yellow-orange solid precipitated out. The reaction was filtered, and the filtrate was collected and lyophilized. The residue was redissolved in methanol and purified via HPLC to give the desired product, SI-2, as a yellow-orange solid. MS: m/z 599.5 $(M+1)^+$.

SI-2 was suspended in 4 M HCl in dioxane (6 ml) and stirred at room temperature for 3.5 h. The reaction was concentrated *in vacuo*, redissolved in methanol, and purified via HPLC to give the desired product SI-3. MS: m/z 499.4 $(M+1)^+$.

Free amine, SI-3 (37.5 mg, 0.08 mmol) and DIPEA (133.4 µl, 0.77 mmol) were suspended in THF (5 ml). MeCN (1 ml) was added to the reaction to help the solubility of the reaction. FITC (26.7 mg, 0.07 mmol) was then added, and the reaction was stirred at room temperature for 3 h. The reaction was purified directly via HPLC to afford the desired product, FL-FITC as a yellow solid. ^{1}H NMR (500 MHz, DMSO-d_6) d ppm 1.18–1.30 (m, 2 H), 1.56–1.64 (m, 1 H), 1.73–1.82 (m, 2 H), 1.85–2.13 (m, 5 H), 2.31–2.45 (m, 4 H), 3.15–3.21 (m, 6 H), 4.03–4.16 (m, 3 H), 4.32 (s, 1 H), 4.49 (s, 2 H), 6.50–6.72 (m, 17 H), 6.98 (d, J = 7.63 Hz, 1 H), 7.09 (d, J = 8.24 Hz, 1 H), 7.17 (d, J = 8.54 Hz, 1 H), 7.57–7.69 (m, 4 H), 7.70–7.77 (m, 1 H), 8.08–8.25 (m, 3 H), 8.63–8.69 (m, 1 H), 9.07 (s, 1 H), and 9.97 (s, 1 H). MS: m/z 887 $(M+1)^+$.

Free amine, SI-3 (13.8 mg, 0.028 mmol) and DMAP (35.5 mg, 0.289 mmol) were dissolved in DMSO (2 ml). A solution of 5,6-TAMRA succinimidyl ester (10.7 mg, 0.020 mmol) in DMSO (1 ml) was added, and the reaction was stirred at room temperature overnight. The reaction was purified via HPLC to afford the desired product, FL-TAMRA as a dark purple solid. ^{1}H NMR (500 MHz, DMSO-d_6) d ppm 1.13–1.20 (m, 1 H), 1.23 (s, 1 H), 1.77–1.84 (m, 1 H), 1.85–1.93 (m, 2 H), 1.93–2.01 (m, 1 H), 2.04–2.18 (m, 1 H), 2.36 (s, 1 H), 2.42 (t, J = 7.32 Hz, 2 H), 3.26 (s, 17 H), 4.10 (t, J = 5.95 Hz, 3 H), 4.29–4.42 (m, 1 H), 4.48 (s, 2 H), 5.73–5.77 (m, 1 H), 5.93–5.97 (m, 1 H), 6.52–6.58 (m, 1 H), 6.60–6.68 (m, 2 H), 6.95 (s, 2 H), 7.00–7.11 (m, 6 H), 7.54–7.69 (m, 4 H), 7.85–7.96 (m, 1 H), 8.11–8.15 (m, 1 H), 8.17 (d, J = 7.93 Hz, 1 H), 8.20–8.25 (m, 1 H), 8.29 (dd, J = 7.93, 1.83 Hz, 2 H), 8.62–8.72 (m, 2 H), 8.75–8.82 (m, 1 H), 8.92 (s, 1 H), 9.06 (s, 1 H), and 9.97 (s, 1 H). MS: m/z 911.8 $(M+1)^+$.

Synthesis of Thap-biotin (Fig. S3). To a solution of Thap-OH (17 mg) in DMSO (1.6 ml) was added biotin-PEG_2-COOH acid (27 mg, 0.06 mmol), DCC (9.7 mg, 0.077 mmol), and DMAP (3.8 mg, 0.031 mmol). The reaction was stirred at 23°C for 16 h. The reaction mixture was further diluted with methanol and was directly purified by HPLC to afford Thap-biotin as colorless oil (13 mg, 42% yield). MS: m/z $(M+1)^+$: 1144.6.

The compound stability of JQ-FT was assessed by LCMS. Next, we collected cell culture media (supernatant) and protein lysates of ALL/SIL cells treated with 20 µM of JQ-FT or 20 µM Thap-OH. In protein lysates of JQ-FT–treated cells, we detected the presence of a Thap-OH peak and the disappearance of the JQ-FT peak, indicating intracellular cleavage of the probe (Fig. S4, A–C). In contrast, in cell culture media of treated cells, we observed the presence of a JQ-FT peak and the lack of a Thap-OH peak, indicating the absence of spontaneous cleavage of the probe in in vitro conditions (Fig. S4, D and E).

Online supplemental material

The detailed syntheses of compound Thap-OH, JQ-FT, biotin-Thap, FL-TAMRA, and FL-FITC are described in the Supplemental material. Fig. S1 describes the synthesis of JQ-FT. Fig. S2 summarizes the synthesis of fluorescence FA derivatives FL-FITC and FL-TAMRA. Fig. S3 describes the synthesis of Thap-biotin. Fig. S4 depicts the LC-MS traces of T-ALL cell line (ALL/SIL) treated with JQ-FT and Thap-OH.

ACKNOWLEDGMENTS

This work was supported by a SCOR Award from the Leukemia and Lymphoma Society (J.E. Bradner, K. Stegmaier, and J. Qi), the William Lawrence and Blanche Hughes Foundation (K. Stegmaier), the Children's Leukemia Research Association (K. Stegmaier), the National Cancer Institute (R35 CA210030), the Claudia Adams Barr Program in Cancer Research (G. Roti and K. Stegmaier), Fondazione Umberto Veronesi (G. Roti), and Associazione Italiana per la Ricerca sul Cancro (n. 17107; G. Roti).

J.E. Bradner is now the President of the Novartis Institutes for Biomedical Research. The other authors declare no competing financial interests.

Author contributions: G. Roti, J. Qi, J.E. Bradner, and K. Stegmaier conceived the project and cowrote the manuscript with input from all coauthors. G. Roti and J. Qi performed the data analysis and interpreted the results. G. Roti, S. Kitara, and A. Su performed the cell-based work. J. Qi, A.C. Varca, and L. Wu designed and synthesized all the probes. M. Sanchez-Martin, A. Saur Conway, A.L. Kung, and A.A. Ferrando performed the in vivo studies and interpreted the results. J.E. Bradner and K. Stegmaier supervised the research.

Submitted: 11 November 2015

Revised: 17 August 2017

Accepted: 9 October 2017

REFERENCES

Ab, O., K.R. Whiteman, L.M. Bartle, X. Sun, R. Singh, D. Tavares, A. LaBelle, G. Payne, R.J. Lutz, J. Pinkas, et al. 2015. IMGN853, a folate receptor-α (FRα)-targeting antibody-drug conjugate, exhibits potent targeted antitumor activity against FRα-expressing tumors. *Mol. Cancer Ther.* 14:1605–1613. https://doi.org/10.1158/1535-7163.MCT-14-1095

Andrews, S.P., M.M. Tait, M. Ball, and S.V. Ley. 2007. Design and total synthesis of unnatural analogues of the sub-nanomolar SERCA inhibitor thapsigargin. *Org. Biomol. Chem.* 5:1427–1436. https://doi.org/10.1039/b702481a

Antony, A.C. 1992. The biological chemistry of folate receptors. *Blood.* 79:2807–2820.

Antony, A.C. 1996. Folate receptors. *Annu. Rev. Nutr.* 16:501–521. https://doi.org/10.1146/annurev.nu.16.070196.002441

Armstrong, D.K., A.J. White, S.C. Weil, M. Phillips, and R.L. Coleman. 2013. Farletuzumab (a monoclonal antibody against folate receptor alpha) in

relapsed platinum-sensitive ovarian cancer. *Gynecol. Oncol.* 129:452–458. https://doi.org/10.1016/j.ygyno.2013.03.002

Armstrong, F., P. Brunet de la Grange, B. Gerby, M.C. Rouyez, J. Calvo, M. Fontenay, N. Boissel, H. Dombret, A. Baruchel, J. Landman-Parker, et al. 2009. NOTCH is a key regulator of human T-cell acute leukemia initiating cell activity. *Blood.* 113:1730–1740. https://doi.org/10.1182/blood-2008-02-138172

Aster, J.C., L. Xu, F.G. Karnell, V. Patriub, J.C. Pui, and W.S. Pear. 2000. Essential roles for ankyrin repeat and transactivation domains in induction of T-cell leukemia by notch1. *Mol. Cell. Biol.* 20:7505–7515. https://doi.org/10.1128/MCB.20.20.7505-7515.2000

Beverly, L.J., D.W. Felsher, and A.J. Capobianco. 2005. Suppression of p53 by Notch in lymphomagenesis: Implications for initiation and regression. *Cancer Res.* 65:7159–7168. https://doi.org/10.1158/0008-5472.CAN-05-1664

Capobianco, A.J., P. Zagouras, C.M. Blaumueller, S. Artavanis-Tsakonas, and J.M. Bishop. 1997. Neoplastic transformation by truncated alleles of human NOTCH1/TAN1 and NOTCH2. *Mol. Cell. Biol.* 17:6265–6273. https://doi.org/10.1128/MCB.17.11.6265

Christensen, S.B., A. Andersen, J.C. Poulsen, and M. Treiman. 1993. Derivatives of thapsigargin as probes of its binding site on endoplasmic reticulum Ca^{2+} ATPase. Stereoselectivity and important functional groups. *FEBS Lett.* 335:345–348. https://doi.org/10.1016/0014-5793(93)80416-R

Christensen, S.B., A. Andersen, H. Kromann, M. Treiman, B. Tombal, S. Denmeade, and J.T. Isaacs. 1999. Thapsigargin analogues for targeting programmed death of androgen-independent prostate cancer cells. *Bioorg. Med. Chem.* 7:1273–1280. https://doi.org/10.1016/S0968-0896(99)00074-7

Christensen, S.B., D.M. Skytte, S.R. Denmeade, C. Dionne, J.V. Møller, P. Nissen, and J.T. Isaacs. 2009. A Trojan horse in drug development: Targeting of thapsigargins towards prostate cancer cells. *Anticancer. Agents Med. Chem.* 9:276–294. https://doi.org/10.2174/1871520610909030276

Dail, M., Q. Li, A. McDaniel, J. Wong, K. Akagi, B. Huang, H.C. Kang, S.C. Kogan, K. Shokat, L. Wolff, et al. 2010. Mutant Ikzf1, KrasG12D, and Notch1 cooperate in T lineage leukemogenesis and modulate responses to targeted agents. *Proc. Natl. Acad. Sci. USA.* 107:5106–5111. https://doi.org/10.1073/pnas.1001064107

Deangelo, D.S.R., and L. Silverman. 2006. A phase I clinical trial of the notch inhibitor MK-0752 in patients with T-cell acute lymphoblastic leukemia/lymphoma (T-ALL) and other leukemias. *J. Clin. Oncol.* 24:357s.

de Figueiredo, R.C., and M.J. Soares. 2000. Low temperature blocks fluid-phase pinocytosis and receptor-mediated endocytosis in Trypanosoma cruzi epimastigotes. *Parasitol. Res.* 86:413–418. https://doi.org/10.1007/s004360050686

Di Ianni, M., S. Baldoni, E. Rosati, R. Ciurnelli, L. Cavalli, M.F. Martelli, P. Marconi, I. Screpanti, and F. Falzetti. 2009. A new genetic lesion in B-CLL: A NOTCH1 PEST domain mutation. *Br. J. Haematol.* 146:689–691. https://doi.org/10.1111/j.1365-2141.2009.07816.x

Doan, N.T., E.S. Paulsen, P. Sehgal, J.V. Møller, P. Nissen, S.R. Denmeade, J.T. Isaacs, C.A. Dionne, and S.B. Christensen. 2015. Targeting thapsigargin towards tumors. *Steroids.* 97:2–7. https://doi.org/10.1016/j.steroids.2014.07.009

Dotto, G.P. 2008. Notch tumor suppressor function. *Oncogene.* 27:5115–5123. https://doi.org/10.1038/onc.2008.225

Ellisen, L.W., J. Bird, D.C. West, A.L. Soreng, T.C. Reynolds, S.D. Smith, and J. Sklar. 1991. TAN-1, the human homolog of the Drosophila notch gene, is broken by chromosomal translocations in T lymphoblastic neoplasms. *Cell.* 66:649–661. https://doi.org/10.1016/0092-8674(91)90111-B

Farber, S., and L.K. Diamond. 1948. Temporary remissions in acute leukemia in children produced by folic acid antagonist, 4-aminopteroyl-glutamic acid. *N. Engl. J. Med.* 238:787–793. https://doi.org/10.1056/NEJM194806032382301

Garin-Chesa, P., I. Campbell, P.E. Saigo, J.L. Lewis Jr., L.J. Old, and W.J. Rettig. 1993. Trophoblast and ovarian cancer antigen LK26. Sensitivity and specificity in immunopathology and molecular identification as a folate-binding protein. *Am. J. Pathol.* 142:557–567.

Girard, L., Z. Hanna, N. Beaulieu, C.D. Hoemann, C. Simard, C.A. Kozak, and P. Jolicoeur. 1996. Frequent provirus insertional mutagenesis of Notch1 in thymomas of MMTVD/myc transgenic mice suggests a collaboration of c-myc and Notch1 for oncogenesis. *Genes Dev.* 10:1930–1944. https://doi.org/10.1101/gad.10.15.1930

Hasserjian, R.P., J.C. Aster, F. Davi, D.S. Weinberg, and J. Sklar. 1996. Modulated expression of notch1 during thymocyte development. *Blood.* 88:970–976.

Herzog, T.J., M.A. Powell, J.S. Rader, R.K. Gibb, L. Lippmann, R.L. Coleman, and D.G. Mutch. 2008. Phase II evaluation of topotecan and navelbine in patients with recurrent ovarian, fallopian tube or primary peritoneal cancer. *Gynecol. Oncol.* 111:467–473. https://doi.org/10.1016/j.ygyno.2008.08.005

Hua, S., H. Malak, J.R. Lakowicz, and G. Inesi. 1995. Synthesis and interaction of fluorescent thapsigargin derivatives with the sarcoplasmic reticulum ATPase membrane-bound region. *Biochemistry.* 34:5137–5142. https://doi.org/10.1021/bi00015a026

Jakobsen, C.M., S.R. Denmeade, J.T. Isaacs, A. Gady, C.E. Olsen, and S.B. Christensen. 2001. Design, synthesis, and pharmacological evaluation of thapsigargin analogues for targeting apoptosis to prostatic cancer cells. *J. Med. Chem.* 44:4696–4703. https://doi.org/10.1021/jm010985a

Kalli, K.R., A.L. Oberg, G.L. Keeney, T.J. Christianson, P.S. Low, K.L. Knutson, and L.C. Hartmann. 2008. Folate receptor alpha as a tumor target in epithelial ovarian cancer. *Gynecol. Oncol.* 108:619–626. https://doi.org/10.1016/j.ygyno.2007.11.020

Katsaros, D., M.V. Oletti, I.A. Rigault de la Longrais, A. Ferrero, A. Celano, S. Fracchioli, M. Donadio, R. Passera, L. Cattel, and C. Bumma. 2005. Clinical and pharmacokinetic phase II study of pegylated liposomal doxorubicin and vinorelbine in heavily pretreated recurrent ovarian carcinoma. *Ann. Oncol.* 16:300–306. https://doi.org/10.1093/annonc/mdi055

Kelemen, L.E. 2006. The role of folate receptor alpha in cancer development, progression and treatment: Cause, consequence or innocent bystander? *Int. J. Cancer.* 119:243–250. https://doi.org/10.1002/ijc.21712

Kridel, R., B. Meissner, S. Rogic, M. Boyle, A. Telenius, B. Woolcock, J. Gunawardana, C. Jenkins, C. Cochrane, S. Ben-Neriah, et al. 2012. Whole transcriptome sequencing reveals recurrent NOTCH1 mutations in mantle cell lymphoma. *Blood.* 119:1963–1971. https://doi.org/10.1182/blood-2011-11-391474

Kularatne, S.A., and P.S. Low. 2010. Targeting of nanoparticles: Folate receptor. *Methods Mol. Biol.* 624:249–265. https://doi.org/10.1007/978-1-60761-609-2_17

Lawrence, M.S., P. Stojanov, C.H. Mermel, J.T. Robinson, L.A. Garraway, T.R. Golub, M. Meyerson, S.B. Gabriel, E.S. Lander, and G. Getz. 2014. Discovery and saturation analysis of cancer genes across 21 tumour types. *Nature.* 505:495–501. https://doi.org/10.1038/nature12912

Leamon, C.P., and P.S. Low. 1991. Delivery of macromolecules into living cells: a method that exploits folate receptor endocytosis. *Proc. Natl. Acad. Sci. USA.* 88:5572–5576. https://doi.org/10.1073/pnas.88.13.5572

Leamon, C.P., and P.S. Low. 1994. Selective targeting of malignant cells with cytotoxin-folate conjugates. *J. Drug Target.* 2:101–112. https://doi.org/10.3109/10611869409015898

Leamon, C.P., M.A. Parker, I.R. Vlahov, L.C. Xu, J.A. Reddy, M. Vetzel, and N. Douglas. 2002. Synthesis and biological evaluation of EC20: A new folate-derived, (99m)Tc-based radiopharmaceutical. *Bioconjug. Chem.* 13:1200–1210. https://doi.org/10.1021/bc0200430

Leamon, C.P., J.A. Reddy, R. Dorton, A. Bloomfield, K. Emsweller, N. Parker, and E. Westrick. 2008. Impact of high and low folate diets on tissue folate receptor levels and antitumor responses toward folate-drug conjugates.

J. Pharmacol. Exp. Ther. 327:918–925. https://doi.org/10.1124/jpet.108.143206

Lee, R.J., and P.S. Low. 1994. Delivery of liposomes into cultured KB cells via folate receptor-mediated endocytosis. *J. Biol. Chem.* 269:3198–3204.

Lobry, C., P. Oh, and I. Aifantis. 2011. Oncogenic and tumor suppressor functions of Notch in cancer: It's NOTCH what you think. *J. Exp. Med.* 208:1931–1935. https://doi.org/10.1084/jem.20111855

Low, P.S., and S.A. Kularatne. 2009. Folate-targeted therapeutic and imaging agents for cancer. *Curr. Opin. Chem. Biol.* 13:256–262. https://doi.org/10.1016/j.cbpa.2009.03.022

Lynn, R.C., M. Poussin, A. Kalota, Y. Feng, P.S. Low, D.S. Dimitrov, and D.J. Powell Jr. 2015. Targeting of folate receptor β on acute myeloid leukemia blasts with chimeric antigen receptor-expressing T cells. *Blood.* 125:3466–3476. https://doi.org/10.1182/blood-2014-11-612721

Lytton, J., M. Westlin, and M.R. Hanley. 1991. Thapsigargin inhibits the sarcoplasmic or endoplasmic reticulum Ca-ATPase family of calcium pumps. *J. Biol. Chem.* 266:17067–17071.

Mamdouh, Z., M.C. Giocondi, R. Laprade, and C. Le Grimellec. 1996. Temperature dependence of endocytosis in renal epithelial cells in culture. *Biochim. Biophys. Acta.* 1282:171–173. https://doi.org/10.1016/0005-2736(96)00077-6

Matherly, L.H., Z. Hou, and Y. Deng. 2007. Human reduced folate carrier: Translation of basic biology to cancer etiology and therapy. *Cancer Metastasis Rev.* 26:111–128. https://doi.org/10.1007/s10555-007-9046-2

Nielsen, S.F., O. Thastrup, R. Pedersen, C.E. Olsen, and S.B. Christensen. 1995. Structure-activity relationships of analogues of thapsigargin modified at O-11 and O-12. *J. Med. Chem.* 38:272–276. https://doi.org/10.1021/jm00002a009

Pan, X.Q., X. Zheng, G. Shi, H. Wang, M. Ratnam, and R.J. Lee. 2002. Strategy for the treatment of acute myelogenous leukemia based on folate receptor beta-targeted liposomal doxorubicin combined with receptor induction using all-trans retinoic acid. *Blood.* 100:594–602. https://doi.org/10.1182/blood.V100.2.594

Parker, N., M.J. Turk, E. Westrick, J.D. Lewis, P.S. Low, and C.P. Leamon. 2005. Folate receptor expression in carcinomas and normal tissues determined by a quantitative radioligand binding assay. *Anal. Biochem.* 338:284–293. https://doi.org/10.1016/j.ab.2004.12.026

Paulos, C.M., J.A. Reddy, C.P. Leamon, M.J. Turk, and P.S. Low. 2004a. Ligand binding and kinetics of folate receptor recycling in vivo: Impact on receptor-mediated drug delivery. *Mol. Pharmacol.* 66:1406–1414. https://doi.org/10.1124/mol.104.003723

Paulos, C.M., M.J. Turk, G.J. Breur, and P.S. Low. 2004b. Folate receptor-mediated targeting of therapeutic and imaging agents to activated macrophages in rheumatoid arthritis. *Adv. Drug Deliv. Rev.* 56:1205–1217. https://doi.org/10.1016/j.addr.2004.01.012

Penton, A.L., L.D. Leonard, and N.B. Spinner. 2012. Notch signaling in human development and disease. *Semin. Cell Dev. Biol.* 23:450–457. https://doi.org/10.1016/j.semcdb.2012.01.010

Procida, K., C. Caspersen, H. Kromann, S.B. Christensen, and M. Treiman. 1998. ACTA, a fluorescent analogue of thapsigargin, is a potent inhibitor and a conformational probe of skeletal muscle Ca2+-ATPase. *FEBS Lett.* 439:127–132. https://doi.org/10.1016/S0014-5793(98)01352-0

Puente, X.S., M. Pinyol, V. Quesada, L. Conde, G.R. Ordóñez, N. Villamor, G. Escaramis, P. Jares, S. Beà, M. González-Díaz, et al. 2011. Whole-genome sequencing identifies recurrent mutations in chronic lymphocytic leukaemia. *Nature.* 475:101–105. https://doi.org/10.1038/nature10113

Punnonen, E.L., K. Ryhänen, and V.S. Marjomäki. 1998. At reduced temperature, endocytic membrane traffic is blocked in multivesicular carrier endosomes in rat cardiac myocytes. *Eur. J. Cell Biol.* 75:344–352. https://doi.org/10.1016/S0171-9335(98)80067-8

Reddy, J.A., R. Dorton, E. Westrick, A. Dawson, T. Smith, L.C. Xu, M. Vetzel, P. Kleindl, I.R. Vlahov, and C.P. Leamon. 2007. Preclinical evaluation of EC145, a folate-vinca alkaloid conjugate. *Cancer Res.* 67:4434–4442. https://doi.org/10.1158/0008-5472.CAN-07-0033

Rijnboutt, S., G. Jansen, G. Posthuma, J.B. Hynes, J.H. Schornagel, and G.J. Strous. 1996. Endocytosis of GPI-linked membrane folate receptor-α. *J. Cell Biol.* 132:35–47. https://doi.org/10.1083/jcb.132.1.35

Ross, J.F., H. Wang, F.G. Behm, P. Mathew, M. Wu, R. Booth, and M. Ratnam. 1999. Folate receptor type beta is a neutrophilic lineage marker and is differentially expressed in myeloid leukemia. *Cancer.* 85:348–357. https://doi.org/10.1002/(SICI)1097-0142(19990115)85:2<348::AID-CNCR12>3.0.CO;2-4

Rothberg, K.G., Y.S. Ying, J.F. Kolhouse, B.A. Kamen, and R.G. Anderson. 1990. The glycophospholipid-linked folate receptor internalizes folate without entering the clathrin-coated pit endocytic pathway. *J. Cell Biol.* 110:637–649. https://doi.org/10.1083/jcb.110.3.637

Rothenberg, M.L., P.Y. Liu, S. Wilczynski, W.A. Nahhas, G.L. Winakur, C.S. Jiang, C.M. Moinpour, B. Lyons, G.R. Weiss, J.H. Essell, et al. 2004. Phase II trial of vinorelbine for relapsed ovarian cancer: A Southwest Oncology Group study. *Gynecol. Oncol.* 95:506–512. https://doi.org/10.1016/j.ygyno.2004.09.004

Roti, G., A. Carlton, K.N. Ross, M. Markstein, K. Pajcini, A.H. Su, N. Perrimon, W.S. Pear, A.L. Kung, S.C. Blacklow, et al. 2013. Complementary genomic screens identify SERCA as a therapeutic target in NOTCH1 mutated cancer. *Cancer Cell.* 23:390–405. https://doi.org/10.1016/j.ccr.2013.01.015

Shen, F., H. Wang, X. Zheng, and M. Ratnam. 1997. Expression levels of functional folate receptors alpha and beta are related to the number of N-glycosylated sites. *Biochem. J.* 327:759–764. https://doi.org/10.1042/bj3270759

Takebe, N., L. Miele, P.J. Harris, W. Jeong, H. Bando, M. Kahn, S.X. Yang, and S.P. Ivy. 2015. Targeting Notch, Hedgehog, and Wnt pathways in cancer stem cells: Clinical update. *Nat. Rev. Clin. Oncol.* 12:445–464. https://doi.org/10.1038/nrclinonc.2015.61

Tanigaki, K., and T. Honjo. 2007. Regulation of lymphocyte development by Notch signaling. *Nat. Immunol.* 8:451–456. https://doi.org/10.1038/ni1453

Thomas, A., J. Maltzman, and R. Hassan. 2013. Farletuzumab in lung cancer. *Lung Cancer.* 80:15–18. https://doi.org/10.1016/j.lungcan.2012.12.021

van Es, J.H., M.E. van Gijn, O. Riccio, M. van den Born, M. Vooijs, H. Begthel, M. Cozijnsen, S. Robine, D.J. Winton, F. Radtke, and H. Clevers. 2005. Notch/gamma-secretase inhibition turns proliferative cells in intestinal crypts and adenomas into goblet cells. *Nature.* 435:959–963. https://doi.org/10.1038/nature03659

Varghese, B., E. Vlashi, W. Xia, W. Ayala Lopez, C.M. Paulos, J. Reddy, L.C. Xu, and P.S. Low. 2014. Folate receptor-β in activated macrophages: Ligand binding and receptor recycling kinetics. *Mol. Pharm.* 11:3609–3616. https://doi.org/10.1021/mp500348e

Vergote, I., and C.P. Leamon. 2015. Vintafolide: A novel targeted therapy for the treatment of folate receptor expressing tumors. *Ther. Adv. Med. Oncol.* 7:206–218. https://doi.org/10.1177/1758834015584763

Wang, H., X. Zheng, F.G. Behm, and M. Ratnam. 2000. Differentiation-independent retinoid induction of folate receptor type beta, a potential tumor target in myeloid leukemia. *Blood.* 96:3529–3536.

Wang, Z., T.G. Da Silva, K. Jin, X. Han, P. Ranganathan, X. Zhu, A. Sanchez-Mejias, F. Bai, B. Li, D.L. Fei, et al. 2014. Notch signaling drives stemness and tumorigenicity of esophageal adenocarcinoma. *Cancer Res.* 74:6364–6374. https://doi.org/10.1158/0008-5472.CAN-14-2051

Weng, A.P., A.A. Ferrando, W. Lee, J.P. Morris IV, L.B. Silverman, C. Sanchez-Irizarry, S.C. Blacklow, A.T. Look, and J.C. Aster. 2004. Activating mutations of NOTCH1 in human T cell acute lymphoblastic leukemia. *Science.* 306:269–271. https://doi.org/10.1126/science.1102160

Whetstine, J.R., R.M. Flatley, and L.H. Matherly. 2002. The human reduced folate carrier gene is ubiquitously and differentially expressed in normal human tissues: Identification of seven non-coding exons and characterization of a novel promoter. *Biochem. J.* 367:629–640. https://doi.org/10.1042/bj20020512

Yanagawa, S., J.S. Lee, K. Kakimi, Y. Matsuda, T. Honjo, and A. Ishimoto. 2000. Identification of Notch1 as a frequent target for provirus insertional mutagenesis in T-cell lymphomas induced by leukemogenic mutants of mouse mammary tumor virus. *J. Virol.* 74:9786–9791. https://doi.org/10.1128/JVI.74.20.9786-9791.2000